3. RESULTS AND DISCUSSIONS

Petroleum is a product whose composition varies due to its natural origins and to transportation and storage conditions. In some origins, petroleum comes from a variety of different oil fields that produce predominantly heavy petroleum.

The demand for high value petroleum products such as middle distillates, gasoline, and lube oils is increasing, while the demand for low value products such as fuel oil and residua based products is decreasing. Therefore, maximizing of liquid products yield from various processes and valorization residues is of immediate attention to refiners. At the same time environmental concerns have increased, resulting in more rigorous specifications for petroleum products, including fuel oils. These trends emphasized the importance of processes that convert the heavier oil fractions into lighter and more valuable clean products [(118)]. A number of technologies have been developed over the years for residual oil upgrading, which include process that are based on the carbon rejection route and hydrogen addition route [(48)].

Large proportions of crudes processed in oil refineries are set aside as distillation residue. At present these residue are of relatively little commercial value. More detailed structural characterizations are necessary before improved process routes to upgrade these materials can even be contemplated.

3.1. Physico-chemical Properties of the Residues and their Constituents:

Physico-chemical properties of the residues and their maltenes separated by different solvents have been determined using ASTM and/or IP standard methods. The results are given in Tables 2 and 5.

The Physico-chemical properties of the studied residues (Table 2) show that these residues are high in density, viscosity and pour point. The results also reveal that these residues have high contents of sulphur, nitrogen, nickel and vanadium.

The results of the physico-chemical properties of the maltenes (Table 5) show that the density and viscosity of the maltenes are less than that of the corresponding residues. The results are also revealing that the sulphur, nitrogen, nickel and vanadium contents in the maltenes are less than that of the corresponding residues. On the other hand, wax content in the maltenes is high than that in the residues. This indicates that the sulphur, nitrogen, nickel and vanadium elements are more concentrated in the asphaltenes, while the paraffinic compounds are concentrated in the maltenes.

The results of the physico-chemical properties of the maltenes also show that the sulphur, nitrogen, nickel and vanadium contents of the maltenes separated by ethyl acetate solvent are less than that of maltenes separated by *n*-heptane solvent, while the wax content has reverse trend

3.2. Composition of the Studied Vacuum Residues:

The two under studied residues were analyzed in order to know how much they contain saturates, aromatic, resins, and asphaltenes. The resultes are given in Table 3 and illustrated in figure 5 and 6. From Table-3 one can see the following:

1- The two Vacuum Residues (VR) contain high percentage of aromatics over both saturates and resins. The order of the percentage of the three components is as follows, whatever the solvent used: aromatics > resins > saturates.

2- The Vacuum Residue from Suez has high aromatic content than that in Alexandria Vacuum Residue. On the other hand, Alexandria Vacuum Residue has higher percentage of both saturates and resins over those in Suez one.

3- The asphaltenes content of Alexandria vacuum residue is higher than that of Suez vacuum residue.

4- In the two studied residues the yield of the asphaltenes separated by ethyl acetate solvent is higher than that separated by *n*-heptane solvent. This indicates that ethyl acetate is more efficient for the separation of the asphaltenes than *n*-heptane.

The data in Table-3 also shows the distribution of hydrocarbons as saturates (*n*-paraffins and cyclic compounds) and aromatics (mono-, di-, and poly). It is clear that *n*-heptane is less efficient for the separation of asphaltenes than *n*-pentane. On the other hand, *n*-heptane gives good results than ethyl acetate and n-pentane for the separation of Maltenes. These data are fully agreed with the data given by H. Alboudwarej and others [(69)], who stated that if higher-carbon-number alkanes are used, less asphaltenes are separated.

3.3. Gas Chromatographic Analysis of the Separated Saturates:

The saturates separated from maltenes by different solvents were subjected to gas chromatographic analysis, and the data are shown in Table-7. From the Table-3 we can see that the saturates separated from maltenes of Alexandria vacuum residue, show higher percentage than that separated from Suez vacuum residue.

Figures (11-15) show the gas chromatograms of the saturates separated from both vacuum residues by different solvents. The chromatograms indicate that the saturates are formed from the resolved components (*n*- and iso-paraffins), and the hump, which is the unresolved complex mixture of naphthenes. The *n*-paraffin distribution of all the saturates separated ranges from about C_{20} to about C_{40} in addition of some traces lighter than C_{20} and higher than C_{40}.

As shown from Table-7, the maximum percentages of *n*-paraffins were separated using *n*-heptane (14.65 % from Alexandria vacuum residue and 13.7 % from Suez vacuum residue). The Table also shows that although ethyl acetate is

less efficient for the separation of *n*-paraffins, it is more efficient than *n*-Pentane which was used in the case of Alexandria vacuum residue only.

3.4. Infrared Studies

The usefulness of infrared spectroscopy lies not only in the detailed information which can be obtained for small molecules, but also, for organic molecules, in the rapid and fairly inexpensive technique it provides for deciding which functional groups are present in a molecule. It has some advantages over mass spectra and nuclear magnetic resonance (NMR), thus, compared with the former it has the advantages that it can be easily applied to no-volatile samples.

Compared to nuclear magnetic resonance, it possesses the ability to give information about all the atoms in the molecule, not just those nuclei with magnetic moments. In practice all the three techniques, and also the ultraviolet spectroscopy, can usually be used to complement each other in a complete diagnosis. Further, infrared spectroscopy does find applications not only for structure determination, but also can be employed for the rapid quantitative analysis of the components of a mixture.

Infrared absorption spectroscopy can be applied for the investigation of the structure of petroleum and its fractions including their functional groups [130-133]. The assignments of the vibration of the function groups, which give rise to their bands in the infrared spectra of the petroleum fractions, are summarized in Table 6.

In this work, the infrared spectra of the two vacuum residues, asphaltenes and maltenes, separated by different solvents, as will as the resins, aromatics and saturates that separated from maltenes by alumina column chromatography, have been measured using FT-IR spectroscopic technique. The residues, maltenes, asphaltenes and resins were measured using the KBr disk technique while the aromatics and saturates were measured in the pure state. The measured infrared spectra in the range 4000 cm^{-1} – 400 cm^{-1} are shown Figures 16-28. The wave-number positions and their corresponding absorbance intensities are shown in Tables (8 - 14).

The infrared spectra of the *n*-heptane and ethyl acetate asphaltenes separated from Suez and Alexandria Vacuum residues are shown in Figures (19 and 20), Table 9.

It is clear that low intensity bands in the region 3500 cm^{-1}–3300 cm^{-1}, with maxima at 3446 cm^{-1} – 3421 cm^{-1} as appeared in the spectra of the Suez vacuum residue, while appeared with maxima at 3451 cm^{-1}– 3419 cm^{-1} in the spectra of Alexandria vacuum residue. These two bands indicate very low concentration of OH and NH groups, which are responsible for asphaltenes aggregation through hydrogen bonding [134]. The very weak bands around 3050 cm^{-1} and 3040 cm^{-1}, result from C-H stretching in aromatic rings. The spectra also reveal strong bands in the region around 3000 cm^{-1} and 2800 cm^{-1}, particularly two distinct bands at about 2920 cm^{-1}. These two bands result from the CH_2 asymmetric and symmetric stretching, respectively. A small peak at about 1693 cm^{-1} in the spectra of asphaltenes may indicate the presence of the carbonyl group (C=O) stretching. All the infrared spectra also show an intense, fairly sharp, band at about 1600 cm^{-1} – 1500 cm^{-1}, which is characteristic of the C=C stretching in aromatic rings. Another strong band observed was also observed around 1461 cm^{-1} – 1451 cm^{-1}, which is due to asymmetric deformation of methyl and methylene groups. A small band observed at about 1375 cm^{-1} might be attributed to methyl symmetric deformation. The band at about 1315 cm^{-1} – 1305 cm^{-1} is due to CH_2 wagging in long chain paraffins. The appearance of a weak band at 1035 cm^{-1} – 1020 cm^{-1} results from the aliphatic C-O, C-N and / or S=O stretching. A very weak band at about 935 cm^{-1} – 906 cm^{-1} may be due to the OH out-of-plane deformation. Three bands at 865 cm^{-1} – 855 cm^{-1}, 810 cm^{-1} and 740 cm^{-1} are weak and broad, and probably result from the out-of-plane deformation of CH in aromatic rings. A weak band at about 720 cm^{-1}, due to CH_2 rocking in long chains $\{-(CH_2)-\}$ where $n \geq 4$, is also present.

The infrared spectra of *n*-heptane and ethyl acetate resins, illustrated in Figures 21and 22 and the data are shown in Table 13, indicate that these resins

have nearly the same functional groups as present in asphaltenes. The spectra show broad bands of OH and NH in the region 3600 cm^{-1} – 3200 cm^{-1} with maxima at about 3419 cm^{-1} in Suez *n*-heptane resin and Alexandria *n*-heptane resin 3415 cm^{-1} or 3370 cm^{-1}. A weak band at 3051 cm^{-1} – 3018 cm^{-1} of CH stretching in aromatic rings, and two strong bands at about 2921 cm^{-1} and 2851 cm^{-1} of the CH_2 asymmetric and symmetric stretching, respectively. A weak band is assigned to the stretching in the carbonyl group at 1685 cm^{-1} – 1648 cm^{-1} [Alexandria resins ethyl acetate], or 1693 cm^{-1} – 1650 cm^{-1} [Alexandria resins *n*-heptane] and 1649 cm^{-1} in case of ethyl acetate Suez resins, while the band at about 1609 cm^{-1} – 1545 cm^{-1} is due to the stretching vibration of C=C aromatic rings. Bands at 1452 cm^{-1}, 1375 cm^{-1} – 1375 cm^{-1} and 1313 cm^{-1} – 1311 cm^{-1} are due to CH_2 plus CH_3 asymmetric deformation, CH_3 symmetric deformation and CH_2 wagging in long chain paraffins, respectively. The band of C-O, C-N or S=O stretching is present at about 1020 cm^{-1}, while that of the OH out-of-plane deformation band is at about 912 cm^{-1} – 914 cm^{-1}. The CH aromatics out-of- plane deformation bands are at about 863–840 cm^{-1}, 811–808 cm^{-1} and 745 cm^{-1}. The band of CH_2 rocking in long chains is also present at about 722 cm^{-1}.

Infrared spectra of the *n*-heptane and ethyl acetate aromatics, mono-aromatics, di-aromatics and poly-aromatics are shown in Figures 23, 24, 27 and 28 and the data are given in Tables 12 and 14. The OH and NH stretching are very weak above 3200 cm^{-1} with maxima at 3556cm^{-1} – 3455 cm^{-1}. The CH stretching in aromatic rings appear at about 3050 cm^{-1} 3040 cm^{-1} and 3020 cm^{-1} – 3015 cm^{-1}. There are very strong two bands at 2927 cm^{-1} and 2851 cm^{-1}, which are probably due to CH_2 asymmetric and CH_3 symmetric stretching, respectively. Two very weak bands appear only in the spectra of aromatics at about 2727 cm^{-1} and 1889 cm^{-1}, the first may represent CH stretching in aldehydes groups, while the second may be due to the overtones of Polycondenced aromatics. The C=O stretching in carbonyl groups is very weak and appears at 1700 cm^{-1} – 1654 cm^{-1}. The C=C stretching in aromatic rings present as a weak band at about 1600 cm^{-1}

in both Alexandria and Suez. The CH_2 plus CH_3 symmetric and CH_3 symmetric deformation bands at about 1462 cm $^{-1}$ and 1376 cm $^{-1}$, respectively. These two bands are sharp and very strong and followed by a weak band at 1311 cm $^{-1}$ – 1305 cm $^{-1}$ due to the CH_2 wagging in long chain paraffins. The very weak band at about 1206 cm $^{-1}$ – 1088 cm $^{-1}$ is attributed to the [–$(CH_3)_2$ –C], while that at 1032 cm $^{-1}$ – 1030 cm $^{-1}$ may be due to C-O, C-N and / or S=O stretching. The CH in naphthenic rings is present as a very weak band at 960 cm $^{-1}$ – 950 cm $^{-1}$. Three bands at 880 cm $^{-1}$, 865 cm^{-1} and 750 cm $^{-1}$ represent the CH aromatic out-of-plane deformation. The CH_2 rocking in long chains, [-$(CH_2)_n$-] where $n \geq 4$ is present at about 720 cm $^{-1}$.

The infrared spectra of the saturate, which were separated from the maltenes by alumina column chromatography, are shown in Figures 25 and 26 and the data are present in Tables 11. The spectra show very weak broad bands of the OH and NH stretching at about 3100 cm^{-1} and higher. The CH_3 asymmetric, CH_3 symmetric, and CH_2 symmetric, stretching vibrations in aliphatic appear as three very strong bands at 2958 cm $^{-1}$ – 2854 cm $^{-1}$, 2927 cm $^{-1}$ – 2917 cm $^{-1}$ and 2854 cm $^{-1}$, respectively. The C=C stretching in aromatics is present as a weak band at 1606 cm $^{-1}$ – 1503 cm $^{-1}$ indicating that the saturates contain very small amounts of aromatics.

Strong bands at nearly 1460 cm^{-1} and1375 cm^{-1} may be attributed to methyl symmetric deformation (scissoring). A very weak band at 1305 cm^{-1} assigned to symmetric wagging of methylene groups in long chain paraffins. The 1038 cm^{-1} very weak band may be due to C-O, C-N and S=O stretching vibrations.

The presence of two very weak bands at about 890 cm $^{-1}$ – 793 cm $^{-1}$ may be assigned to the out-of-plane deformation of C-H in aromatics. These bands, as well as the band of C=C stretching in aromatics at about 1600 cm $^{-1}$ indicate, also, the presence of very small amounts of aromatic in the separated saturates. The two strong bands at about 730 cm $^{-1}$ may be due to the rocking of methylene groups in long chain paraffins that having four [CH_2] groups or more.

Some ratios calculated from peak heights of selected infrared bands allow for better comparison of the spectra. The ratio of absorbance of CH_3 symmetric deformation at 1375 cm $^{-1}$ to that of CH_2 + CH_3 symmetric deformation at 1460 cm^{-1}, i.e., A_{1375}/A_{1460} is measure of the degree of branching and the ratio of CH_2 rocking at 720 cm $^{-1}$ to CH_2 + CH_3 or CH_3 symmetric deformation, i.e., A_{720}/A_{1460} or A_{720}/A_{1375} is measure of the chain length [135]. The degree of substitution in aromatic structure is measured from the ratio of absorbance of CH aromatic out-of-plane deformation two/thee- or four adjacent hydrogen atoms, at 810 or 750 cm $^{-1}$, respectively, to that of one free hydrogen atom at 870 cm $^{-1}$ [136], i.e., A_{810}/A_{870} or $A_{750}/A_{870.}$

The degree of branching, chain length and the substitution degree in aromatic structures have been determined for asphaltenes, resins and aromatics. The results are given in Table 15. The results show that the degree of branching in asphaltenes separated by *n*-heptane solvents from both Alexandria and Suez residues is more than that separated by ethyl acetate, while the chain length of *n*-heptane asphaltenes is less than that of ethyl acetate asphaltenes. The degree of branching of the resins and aromatics separated by *n*-heptane is less than that of those separated by ethyl acetate and the chain length of *n*-heptane resin and aromatic is more longer than that of ethyl acetate resin and aromatics. The results also reveal that the ratios of A_{810}/A_{870} or A_{750}/A_{870} in the asphaltenes separated by n-heptane are higher than that asphaltenes separated by ethyl acetate. This indicates that the degree of substitution in the aromatics system of the *n*-heptane asphaltenes is less than that of ethyl acetate asphaltenes. On the other hand, the degree of substitution in the aromatics system of n-heptane resins and aromatics is higher than that of ethyl acetate resins and aromatics.

3.5. Ultraviolet Studies:

Ultraviolet spectroscopy is generally employed to study the presence of total, mono-, di- and poly-aromatics in crude petroleum and its fractions.

It is well known that saturates have no significant absorption bands in the ultraviolet or visible spectroscopy. Therefore, the ultraviolet–visible spectroscopy is generally employed for the detection of aromatics [137]. 0n addition to the well defined amounts; of energy to increase its vibrational and rotational energy, a molecule can also absorb some energy to increase the energy of its electrons. The energy changes involved are considerably greater than those involved in vibrational and rotational energy changes and correspond to radiation in the ultraviolet (λ = 200–400 nm) and visible (λ = 400–750 nm).

In our study, the two understudied vacuum residues and their constituents were subjected to ultraviolet / visible study. The data are given in Tables 16 and 17 and the spectra are shown in Figures 29 and 30. From the two Tables, one can see the presence of two prominent bands, one sharp band at the range between about 230 nm to 235 nm, which mainly correspond to the diaromatics, and the other band is strong and appears at about 255 nm, which generally shifted towards higher wavelengths, 256.0 nm – 257.5 nm, as shown by Suez vacuum residue, Table-16, and 254.5 nm – 257.5 nm, as shown by Alexandria vacuum residue, Table-17.

A third band was reported at about 191 nm. This band sometimes shifted to higher wavelength, 191 nm – 198 nm, in the case of the two vacuum residues. Generally the absorption coefficient (α) is higher at λ_2 and λ_3, corresponding to di-aromatics and poly-aromatics respectively, but it is lower in the case of λ_1, which is corresponding to the mono-aromatics.

As shown from the two Tables, mono-aromatics, which were separated by asilica gel column chromatography, reveals three wavelengths at 195 nm *(of intensity coefficient 57.59)*, 232 nm *(of intensity coefficient 43.95)*, and 257 nm *(of intensity coefficient 40.13)* in the case of Suez vacuum residue, but in the case of the Alexandria vacuum residue, these three bands are shown at 194 nm

(of intensity coefficient 130.68), 231 nm *(of intensity coefficient 68.92),* and 256 nm *(of intensity coefficient 51.78),* respectively. The intensities of these bands indicate that mono aromatics separated by column chromatography still contain some traces of both Diaromatics and polyaromatics.

The same is observed in the case of Diaromatics and polyaromatics. The Diaromatics reveals three bands at 191 nm *(of intensity coefficient 36.19),* 231 nm, *(of intensity coefficient103.0),* and 256 nm, *(of intensity coefficient 98.16)* in the case of Suez vacuum residue. On the other hand, Alexandria vacuum residue reveals corresponding three bands at 194 nm *(of intensity coefficient 48.41),* 229.5 nm, *(of intensity coefficient 175.18),* and 257.5 nm, *(of intensity coefficient 96.81).*

The polyaromatics also reveals three absorption bands at 197.5 nm, *(of intensity coefficient 29.79),* 229.5 nm, *(of intensity coefficient 76.49),* and 256.5 nm, *(of intensity coefficient 109.76),* as shown by Suez vacuum residue. These bands revealed by Alexandria vacuum residue at 193.5 nm, *(of intensity coefficient 49.43),* 231 nm, *(of intensity coefficient 72.42),* and 256 nm, *(of intensity coefficient 125.72).*

The above results indicate that the aromatic constituents of the petroleum vacuum residue contain a complex mixture of mono-, di-, and polyaromatics that affect the efficiency of silica gel column chromatography, and therefore, the separated monoaromatics, diaromatics, and polyaromatics each of them contains a trace amount of the two others.

3.6. Elemental Distribution:

Usually, crude oils typically contain trace amounts of metals and nonmetals. Of the nonmetals, sulfur and nitrogen are the most common; vanadium and nickel are the most common metals. Usually these elements are present in the form of oil soluble salts. The nonmetal sulfur is the only one which may occur in the elemental state. In conventional refining processes these elements become concentrated in the residual fractions.

Mohammed and Saeed [127], the physical, chemical and catalytic treatment processes that carried out for the removal of vanadium and nickel which are mostly concentrated in the vacuum residues, specifically in the asphaltenes.

The distribution of the sulphur and nitrogen in the residues among their asphaltenes and maltenes and the distribution of the nickel and vanadium in the residues among their asphaltenes and resins are given in Table 4 and illustrated in Figures 7–10.

Looking in Table- 4, one can see that sulfur is concentrated in Asphaltenes, whatever the solvent used. The Alexandria residue contains the highest amount of sulfur, as present in Asphaltenes, over that of Suez vacuum residue. Alexandria vacuum residue contains 3.83 wt % and 3.65 wt % sulfur as separated using *n*-heptane and ethyl acetate respectively, while the corresponding values in Suez vacuum residue are 3.12 and 2.99, respectively.

On the other hand, the percentage of nitrogen is (0.44 wt %) in the Suez vacuum residue; it is 0.97 wt % and 0.92 wt % as separated by *n*-heptane and ethyl acetate, respectively. In the same time, Alexandria vacuum residue shows higher percentages of nitrogen, they are 2.37 wt % and 2.27 wt % also as separated by *n*-heptane and ethyl acetate, respectively.

Concerning the distribution of sulphur between asphaltenes and maltenes separated by *n*-heptane and ethyl acetate solvents (Table 4 & Figure 7), it is clear that asphaltenes separated by *n*-heptane contain 0.31wt % and 0.24 wt % of the

total sulphur of Alexandria residue (3.09 wt %) and Suez residue (2.89 wt %), respectively and asphaltenes separated by ethyl acetate contain 0.61 wt % and 0.48 wt % of the total sulphur of Alexandria residue and Suez residue, respectively.

Considering the distribution of nitrogen between asphaltenes and maltenes separated by *n*-heptane and ethyl acetate solvents (Table 4 & Figure 8), it is clear that asphaltenes separated by *n*-heptane contain 0.19 wt % and 0.07 wt % of the total nitrogen of Alexandria residue (0.65 wt %) and Suez residue (0.44 wt %), respectively and asphaltenes separated by ethyl acetate contain 0.38 wt % and 0.15 wt % of the total nitrogen of Alexandria residue and Suez residue, respectively.

Vanadium and nickel contents in our studied samples were determined through the sulphuric acid ashing, dissolution in dilute hydrochloric acid and successive measurement using Inductively coupled plasma-atomic emission spectroscopic technique. The results given in Table-4 indicate that the quantity of the two elements separated is highly affected by the solvent used for separation.

The corresponding values of nickel and vanadium contents in the resins are so much lower than that in asphaltenes, but the Suez vacuum residue contains higher amounts over Alexandria vacuum residue.

Among the solvent used, *n*-heptane gave the best results in the case of the two vacuum residues used. n-heptane gave 458.91 ppm and 571.89 ppm nickel in case Alexandria and Suez vacuum residues respectively, while ethyl acetate gave corresponding values as 382.69 ppm and 421.45 ppm, respectively.

The results of vanadium show the same order. Ethyl acetate gave lower vanadium than *n*-heptane. The data obtained from *n*-heptane are 617.26 ppm and 857.56 ppm from Alexandria and Suez vacuum residues respectively, while ethyl acetate gave corresponding values as 469.54 ppm and 616.40 ppm, respectively.

The importance of the metal analysis in the heavy petroleum residues is to decide which suitable catalytic process must be used to upgrade such heavy

fractions. Another important point is the effect of heavy metals on the efficiency of the catalyst used, they not only contaminate the products, their chelates cause poisoning and fouling the catalyst and corrode the equipments.

Regarding the nickel and vanadium distribution between asphaltenes and resins (Table 4 & Figures 9 and 10), the Alexandria *n*-heptane asphaltens contain 37.22 ppm nickel and 50.06 ppm vanadium and Alexandria ethyl acetate asphaltens contain 63.79 ppm nickel and 78.27 ppm vanadium of the total nickel (89.94 ppm) and vanadium (118.23 ppm) of Alexandria residue. The corresponding values of the Suez asphaltenes 43.75 ppm nickel and 65.60 ppm vanadium and 67.97 ppm nickel and 99.42 ppm vanadium of the total nickel (113.45 ppm) and vanadium (145.23 ppm) of the Suez residue. This indicates that ethyl acetate solvent more efficient for removal the sulphur, nitrogen, nickel and vanadium elements from the vacuum residue than *n*-heptane solvent.

Table-1: Typical Fractions Obtained on Distillation of Crude Oil

Output %	Boiling Range, ^{o}C	Carbon Atoms	Product
2	< 30	1 to 4	Light products *
15 – 30	30 – 200	4 to 12	Naphtha
5 to 20	200 – 300	12 to 15	Kerosene
10 to 40	300 – 400	15 to 25	Gas Oil
Residue	400 $^{+}$	25 $^{+}$	Residual Oil

* - Also Known as Light Hydrocarbons

Table-2: Physicochemical Properties of the Studied Samples

Sample Properties	Vacuum Residues	
	From Alexandria	From Suez
Density at 60 °F, g/ml *	1.0050	1.0009
GRAVITY: *		
* Specific, at 60/60 °F	1.0060	1.0019
* API	9.16	9.74
VISCOSITY, cSt at:		
• 50 °C *	23466.83	17072.38
• 80 °C	1658.60	1369.60
• 100 °C	460.50	401.80
Pour Point, °C	+ 48	+ 48
Sulfur Content, wt.	3.09	2.89
Nitrogen, wt %	0.65	0.44
Carbon Residue, wt %	18.19	18.75
Wax Content, wt %	2.89	1.75
Ash, wt %	0.038	0.039
Nickel, ppm	89.94	113.45
Vanadium, ppm	118.23	145.23

* Calculated.

Table-3: Composition of the Two Residues Using Different Solvents

Components, wt %	Alexandria			SUEZ	
	n-Pentane	n-Heptane	Ethyl Acetate	n-Heptane	Ethyl Acetate
Asphaltenes	15.09	8.11	16.67	7.65	16.13
Maltenes	84.91	91.89	83.33	92.35	83.87
*-Saturates	15.28	14.14	15.94	8.63	8.48
*-Aromatics	42.29	41.31	45.45	65.24	62.48
-Mono-		8.73		17.61	
-Di-		16.76		24.02	
-Poly-		15.82		23.61	
Resins	27.34	36.44	21.94	18.48	12.91

N.B.: 1- All the figures in the table are calculated with reference to the residue.

Table – 4: Elemental Distribution of Sulfur, Nitrogen, vanadium and Nickel

The Element, wt %	In Alexandria			In Suez	
	n-Pentane	n-Heptane	Ethyl Acetate	n-Heptane	Ethyl Acetate
Sulfur In:					
Asphaltenes	3.69 (0.57)	3.83 (0.31)	3.65 (0.61)	3.12 (0.24)	2.99(0.48)
Maltenes	2.90 (2.46)	2.98 (2.74)	2.95 (2.46)	2.85 (2.63)	2.81 (2.36)
Nitrogen In:					
Asphaltenes	2.05 (0.31)	2.37 (0.19)	2.27 (0.38)	0.97 (0.07)	0.92 (0.15)
Maltenes	0.40 (0.34)	0.49 (0.45)	0.31 (0.26)	0.40 (0.37)	0.34 (0.28)
Nickel In **:**					
Asphaltenes	414.5 (62.54)	458.91(37.22)	382.69 (63.79)	571.89 (43.75)	421.45 (67.97)
Resins	91.27(24.95)	130.45(47.53)	95.81 (21.02)	320.50 (59.22)	285.36 (36.84)
Vanadium In **:**					
Asphaltenes	514.73 (77.67)	617.26 (50.06)	469.54 (78.27)	857.56 (65.60)	616.40 (99.42)
Resins	132.37 (36.19)	189.92 (67.02)	148.17 (32.51)	389.61(72.00)	311.47 (40.21)

N.B.: 1- The figures between brackets are calculated relative to the residue.

2- Nickel and Vanadium are in ppm.

Table-5: Physicochemical Characteristics of Separated Maltenes

PROPERTIES	Alexandria			Suez	
	n-Pentane	n-Heptane	Ethyl Acetate	n-Heptane	Ethyl Acetate
Density at 60^0 F, g/ml *	0.9815	0.9945	0.9887	0.9876	0.9823
GRAVITY:					
Specific, at $60/60^0$ F *	0.9825	0.9955	0.9897	0.9886	0.9833
^{0}API*	12.53	10.65	11.47	11.63	12.40
VISCOSITY, cSt at:					
• 50^o C *	801.25	1230.77	666.87	1288.07	567.43
• 80^o C	505.84	401.19	220.50	377.17	207.82
• 100^o C	101.91	218.90	122.05	195.94	120.74
Pour Point, ^{o} C	42	45	42	45	39
Sulfur Content, wt.	2.90	2.98	2.95	2.85	2.81
Nitrogen, wt %	0.40	0.49	0.31	0.40	0.34
Carbon Residue, wt %	11.88	13.28	12.83	14.12	12.15
Wax Content, wt %	3.38	3.14	3.47	1.88	2.07
Nickel, ppm	31.93	57.76	31.38	75.17	54.20
Vanadium, ppm	47.69	74.19	47.88	84.71	54.61

* Calculated.

Table-6 Assignment of the Vibrations of the Functional Groups in the Infrared Spectra of the Petroleum Products

Wave numbers, Cm^{-1}	Assignment of the Vibrations of the Functional Groups
3600 - 3200	OH Stretching, NH Stretching,
3100 – 3000	CH Stretching in Aromatic Rings
2955 – 2945	CH_3 asymmetric Stretching
2930 – 2910	CH_2 asymmetric Stretching
2900 – 2880	CH Stretching in CH_3, CH_2, and CH
2875 – 2850	CH_3 Symmetric Stretching
2860 - 2845	CH_2 Symmetric Stretching
2730 - 2725	CH stretching in Aldehyde Groups
2000 – 1800	Overtones of Polycondenced Aromatics
1760 – 1640	C = O Stretching in Carbonyl Groups.
1610 – 1590	C = C Stretching in Aromatic Rings.
1485 – 1445	CH_2 and CH_3 a Symmetric Deformation (Scissoring).
1380 – 1365	CH_3 Symmetric Deformation (Scissoring).
1315 – 1300	CH_2 Wagging in Long Chain Paraffins.
1165 – 1155	$(CH_3)_2 - C$.
1035 - 1020	C – O Stretching, C – N Stretching, S = O Stretching.
970 – 950	CH in naphthenic rings.
945 - 910	OH out-of-plane deformation.
890 – 860	CH aromatic out-of-plane deformation (1 free hydrogen
815 – 805	CH aromatic out-of-plane deformation (2 or 3 adjacent free hydrogen atoms).
760 – 740	CH aromatic out-of-plane deformation (4 adjacent free hydrogen atoms)
730 – 720	CH_2 rocking in chains $-(CH_2)_n$, $n \geq 4$

Table-7 Gas Chromatographic Data of The Saturates Separated From Maltenes By Liquid (Column) Chromatography.

Fraction	Saturates of Alexandria			Saturates of Suez	
	n-Pentane	n-Heptane	Ethyl Acetate	n-Heptane	Ethyl Acetate
n-Paraffins	10.98	14.65	13.04	13.70	12.31
Cyclic compounds	89.02	85.35	86.96	86.30	87.69

Table-8: Infrared Data of the Vacuum Residues Under Studies

Wave Number, Cm^{-1}	Absorbance	
	AVR (a)	SVR (b)
3500 – 3300	0.0574	0.1038
3100	0.0301	0.0617
2950	1.2501	0.8730
2920	1.8030	1.3452
2850	1.3296	1.0084
1600	0.1098	0.1150
1460	0.6060	0.4492
1375	0.3558	0.2687
1310	0.1509	0.1270
1030	0.0745	0.0924
930	0.0334	0.0511
870	0.0678	0.0586
810	0.0854	0.0726
745	0.0872	0.0791
720	0.1151	0.0999

(a) Alexandria Vacuum Residue, (b) Suez Vacuum Residue

Table-9: Infrared Data of the Asphaltenes Extracted By Different Solvents

Wave Number, Cm^{-1}	Absorbance				
	Alexandria			Suez	
	n-Pentane	n-Heptane	Ethyl Acetate	n-Heptane	Ethyl Acetate
3500 – 3300	0.1214	0.0792	0.1205	0.1388	0.1218
3050 - 3040	0.0918	0.0560	0.1045	0.0873	0.1047
2920	1.3156	0.7010	1.4805	1.4473	1.4010
2850	0.9859	0.5390	1.1594	1.1016	1.0994
1750	0.0502	0.0243	0.0525	0.0530	0.0558
1693	0.0485	0.0293	0.0217	0.0531	0.0835
1595	0.2294	0.1128	0.2224	0.2322	0.2374
1450	0.5312	0.2874	0.5979	0.5422	0.5513
1375	0.3969	0.2203	0.4538	0.3984	0.4046
1310	0.2916	0.1693	0.3260	0.2835	0.3052
1030	0.1404	0.0798	0.1257	0.1480	0.1760
930	0.0453	0.0223	0.0468	0.0512	0.0545
860	0.0922	0.0435	0.1076	0.0816	0.0929
808	0.1162	0.0580	0.1310	0.1006	0.1035
745	0.1203	0.0601	0.1221	0.1034	0.1006
720	0.1002	0.0541	0.1149	0.0916	0.1218

Table-10 Infrared Data of the Maltenes Extracted By Different Solvents

Wave Number, Cm^{-1}	Absorbance				
	Alexandria			Suez	
	n-Pentane	n-Heptane	Ethyl Acetate	n-Heptane	Ethyl Acetate
3500 – 3300	0.0822	0.0916	0.0725	0.0902	0.0997
3050 - 3040				0.1702	
2950	1.8198	2.0860	1.7579	1.5268	1.5458
2930	2.2249	2.5276		3.2097	1.9888
2920	2.3299	2.9397	2.3681	2.2159	2.2130
2850	1.8798	2.3552	1.7200	1.8610	1.5669
1750	0.1051	0.0815	0.0399		
1693	0.0733	0.0940	0.0778		
1595	0.1808	0.2411	0.1454	0.1520	0.2162
1460	1.0114	1.1112	0.8996	0.7059	0.7663
1375	0.5962	0.6955	0.5261	0.4094	0.5440
1310	0.2714	0.3305	0.1968	0.1892	0.2932
1030	0.2141	0.2325	0.1182	0.1207	0.2317
928			0.0525	0.463	0.1452
865	0.1760	0.1906	0.1263	0.0826	0.1778
810	0.1930	0.2121	0.1645	0.0949	0.1796
745	0.1764	0.1970	0.1708	0.0892	0.1531
720	0.2164	0.2371	0.1816	0.1139	0.1592

Table-11: Infrared Data of the Saturates Extracted From Maltenes

Wave Number, Cm^{-1}	Absorbance				
	Alexandria			Suez	
	n-Pentane	n-Heptane	Ethyl Acetate.	n- Heptane	Ethyl Acetate
3500 – 3300	0.1060	0.1074	0.1255	0.2053	0.1541
2950	0.5895	1.0932	2.5098	2.0581	1.0015
2920	0.8327	1.8870	1.1355	2.3789	1.5830
2850	0.6279	1.2515	0.5484	1.9672	1.1398
1600	0.0943	0.0957	0.1289	0.1937	0.1405
1460	0.3946	0.5693	0.9144	1.3117	0.6115
1375	0.2535	0.3348	0.4984	0.7176	0.3697
1310	0.1281	0. 1469	0.1510	0.2415	0.1781
1070	0.1211	0.1327	0.1170	0.1778	0.1573
970	0.1080	0.1265	0.1176	0.1786	0.1524
890	0.0896	0.1134	0.1038	0.1576	0.1273
730	0.1431	0.1564	0.2587	0.4430	0.2121
720	0.1616	0.1813	0.3004	0.4990	0.2384

Table-12: Infrared Data of the Aromatics Extracted From Maltenes

Wave Number, Cm^{-1}	Absorbance				
	Alexandria			Suez	
	n-Pentane	n-Heptane	Ethyl Acetate.	n- Heptane	Ethyl Acetate
3500 – 3300	0.7940	0.0455	0.0592	0.0781	0.0934
3050 - 3040					
2950	1.2670	1.0001	1.1991	1.5198	1.1497
2920	1.8665	1.5390	1.7441	1.1615	1.8304
2250	1.3024	1.0576	1.2409	1.5310	1.2084
1750	0.0276				
1700-1660			0.0495	0.0638	
1600	0.1077	0.0786	0.1122	0.1530	0.1171
1450	0.6865	0.5308	0.6445	0.7690	0.5882
1375	0.3971	0.3042	0.3831	0.4615	0.3499
1310	0.1606	0.1261	0.1648	0.2181	0.1622
1030	0.1371	0.1070	0.1262	0.1712	0.1350
930	0.0635	0.0563	0.0690	0.1142	0.1087
860	0.1194	0.0955	0.1127	0.1407	0.1090
808	0.1517	0.1193	0.1428	0.1551	0.1241
745	0.1355	0.1060	0.1283	0.1377	0.1074
720	0.1451	0.1151	0.1297	0.1431	0.1034

Table-13: Infrared Data of the Resins Extracted From Maltenes

Wave Number, Cm^{-1}	Absorbance				
	Alexandria			Suez	
	n-Pentane	n-Heptane	Ethyl Acetate.	n- Heptane	Ethyl Acetate.
3500 – 3300	0.2417	0.1289	0.1316	0.1188	0.1658
3050 - 3040	0.1598	0.0824	0.0479	0.1013	0.1201
2920	1.3635	2.0252	1.7403	2.0287	2.0887
2850	1.1075	1.5124	1.3184	1.5299	4.4710
1700-1660	0.2117	0.1976	0.1191	0.2599	0.3717
1600	0.3096	0.2658	0.2068	0.2912	0.3068
1450	0.6857	0.7233	0.6493	0.7636	0.7407
1375	0.4809	0.4722	0.4319	0.5118	0.4806
1310	0.2928	0.2752	0.2374	0.3186	0.2844
1030	0.2529	0.2216	0.2407	0. 2535	0.2841
930	0.0862	0.0726	0.0498	0.0869	0.0792
860	0.1015	0.0934	0.0680	0.1152	0. 0792
808	0.1287	0.1155	0.0913	0.1360	0.1186
745	0.1571	0.1313	0.1197	0.1502	0.1331
720	0.1109	0.1184	0.1002	0.1440	0.1145

Table-14: Infrared Data of the Mono-, Di-, and Poly-Aromatics

Wave Number, Cm^{-1}	Absorbance					
	Alexandria			Suez		
	Mono-	Di-	Poly-	Mono-	Di-	Poly-
3500-3300	0.1518	0.0264	0.1852	0.1086	0.0571	0.1839
3050			0.2204		0.1046	0.1431
2950	1.9149	0.3963	1.2344	2.4544	1.4017	0.6797
2920	2.7627	0.4103	1.4957	2.7073	2.0532	0.9135
2850	2.1164	0.3946	1.1052	2.2781	1.3222	0.7160
1750-1700		0.0143	0.3462	0.0791		0.1496
1600	0.1722	0.0699	0.2045	0.1414	0.1521	0.1943
1460	1.1132	0.3282	0.6992	1.4253	0.6630	0.4295
1375	0.5582	0.2429	0.4816	0.7451	0.4428	0.3146
1310	0.2323	0.1043	0.3042	0.2015	0.2250	0.2201
1070	0.1949	0.0663	0.2090	0.1330	0.1864	0.1384
920	0.1620	0.0344	0.0773	0.1056	0.1380	0.0743
870	0.1815	0.0868	0.0997	0.1229	0.1583	0.1093
810	0.2082	0.1216	0.1381	0.1623	0.1849	0.1426
745		0.1097	0.1685		0.1416	0.1725
730	0.3480			0.3318		
720	0.3867	0.1092	0.1464	0.3764	0.1130	0.1366

Table-15: Chain Length, Degree Of Branching And Substitution Degree In The Aromatics Structures Of The Asphaltenes, Resins And Aromatics Determined By The Infrared Spectrometry.

Fractions	Chain Length		Degree of Branching	Substitution Degree	
	A_{720}/A_{1375}	A_{720}/A_{1450}	A_{1370}/A_{1450}	A_{810}/A_{870}	A_{750}/A_{870}
Asphaltenes:					
- Alexandria:					
- *n*-Pentane	0.252	0.189	0.747	1.260	1.305
- *n*- Heptane	0.246	0.188	0.767	1.333	1.382
- Ethyl acetate	0.253	0.192	0.759	1.217	1.135
- Suez:					
- *n*- Heptane	0.230	0.169	0.735	1.233	1.267
- Ethyl acetate	0.301	0.221	0.734	1.114	1.083
Resins:					
- Alexandria:					
- *n*-Pentane	0.231	0.162	0.701	1.268	1.548
- *n*- Heptane	0.251	0.164	0.653	1.237	1.406
- Ethyl acetate	0.231	0.154	0.665	1.343	1.760
- Suez:					
- *n*- Heptane	0.281	0.181	0.664	1.181	1.304
- Ethyl acetate	0.238	0.155	0.649	1.497	1.681
Aromatics:					
- Alexandria:					
- *n*-Pentane	0.365	0.211	0.578	1.271	1.135
- *n*- Heptane	0.378	0.217	0.572	1.249	1.110
- Ethyl acetate	0.338	0.201	0.573	1.267	1.138
- Suez:					
- *n*- Heptane	0.310	0.186	0.600	1.102	0.979
- Ethyl acetate	0.295	0.176	0.595	1.138	0.985

Table-16: Ultraviolet Spectra of Suez Vacuum Residue and its Constituents as Separated by different Solvents

Suez Fraction	Monoaromatics		Diaromatics		Polyaromatics	
	λ_1	α_1	λ_2	α_2	λ_3	α_3
Residue	194.5[@]	64.29	235	108.15	254.5	160.92
Maltenes Extracted By:						
n-Heptane.	194.5	60.06	231.5	111.18	257.5	133.16
Ethyl Acetate.	193.0	55.78	230.5	102.03	254.5	110.09
Asphaltene Extracted By:						
n-Heptane.	191.5	78.06	234.0	138..92	251.0	446.57
Ethyl Acetate.	198.5	75.03	234.0	139..63	255.0	390.59
Aromatics Extracted By:						
n-Heptane.	195.0	43.93	227.0	78.03	257.0	86..61
Ethyl Acetate	193.5	39.72	227.5	61.77	257.5	78.96
Resin Extracted By:						
n-Heptane.	198.0	123.82	233.0	262.16	257.0	373.54
Ethyl Acetate	192.0	104.36	234.0	193.72	251.0	305.04
Monoaromatics (†)	195.0	57.59	232.0	43.95	257.5	40.13
Diaromatics (†)	191.0	36.19	231.0	103.00	256.0	98.16
Polyaromatics (†)	197.5	29.79	229.5	76.49	256.5	109.76

α = L g^{-1}.Cm^{-1}, (†): As separated by Column Chromatography.

Table-17: Ultraviolet Spectra of Alexandria Vacuum Residue and its Constituents as Separated by different Solvents

Alexandria Fraction	Monoaromatics		Diaromatics		Polyaromatics	
	λ_1	α_1	λ_2	α_2	λ_3	α_3
Residue	193[@]	54.14	229.5	103.76	253.50	139.48
Maltenes extracted by: n-Heptane. Ethyl Acetate. n-Pentane.	 194.5 192.5 192.0	 54.64 59.04 57.45	 234.0 232.5 228.5	 100.35 108.11 90.42	 257.5 257.5 257.0	 117.88 127.94 121.17
Asphaltenes extracted by: n-Heptane. Ethyl Acetate. n-Pentane.	 194.5 195.5 192.5	 44.32 40.01 39.7	 230.5 230.5 230.5	 127.60 101.21 134.69	 244 258 256	 324.31 210.64 242.70
Aromatics extracted by: n-Heptane. Ethyl Acetate n-Pentane	 191 192 198	 64.17 57.19 60.29	 230.50 235.00 232.00	 105.43 134.14 96.38	 251 258 259	 99.39 133.97 111.47
Resin extracted by: n-Heptane. Ethyl Acetate n-Pentane	 192.0 196.5 194.0	 64.11 80.34 85.47	 232.5 232.0 232.5	 116.25 115.61 113.36	 257.5 257.5 245.0	 193.49 195.15 190.32
Monoaromatics (†) Diaromatics (†) Polyaromatics (†)	194.0 194.0 193.5	130.68 48.41 49.43	231.0 229.5 231.0	68.92 175.18 72.42	256.0 257.5 256.0	51.78 96.81 125.72

α = L g^{-1}.Cm^{-1}, (†): As separated by Column Chromatography.

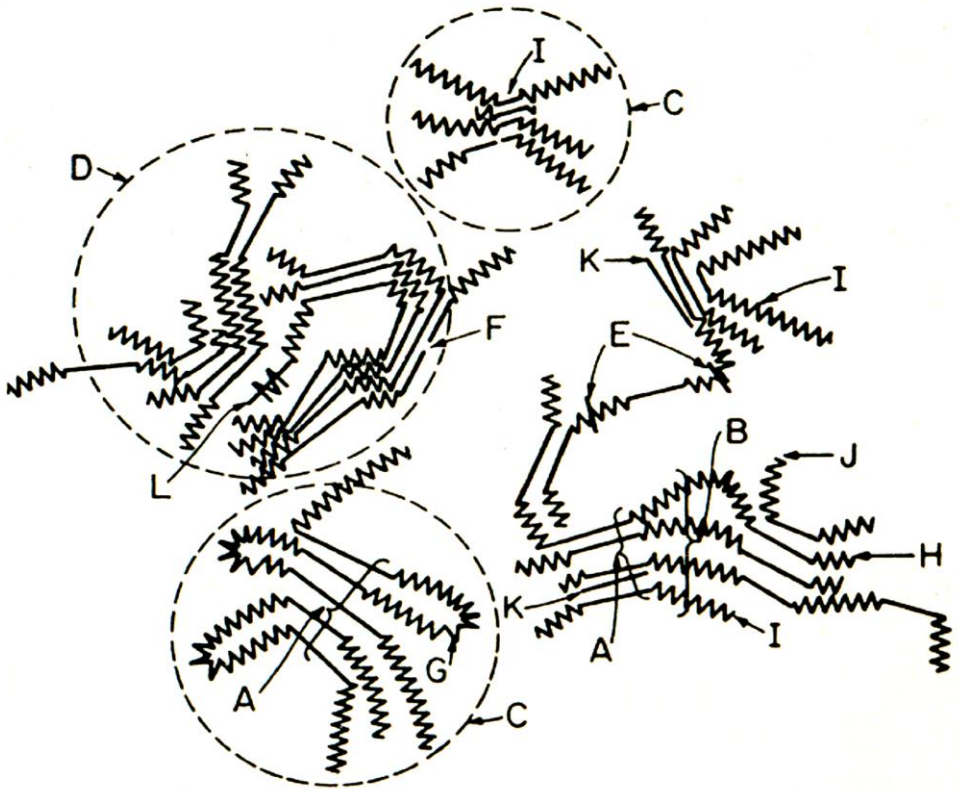

Figure – 1: Macrostructure of Asphaltic: A- Crystalline, B- Chain Bundle, C- Particle, D- Micelle, E- Weak Link, F- Gap and Hole, G- & H- Intercluster, I- Resin, J- Single Layer, K- Petroporphyrins, and L- Metal

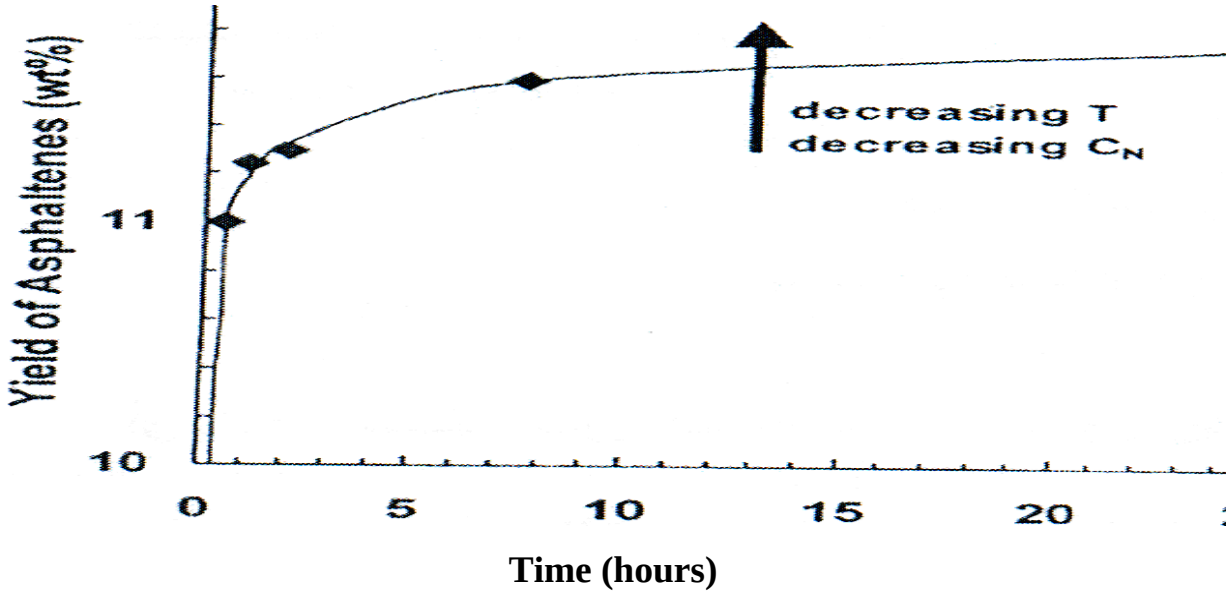

Figure-2: Effect of Time on the Yield of Asphaltenes

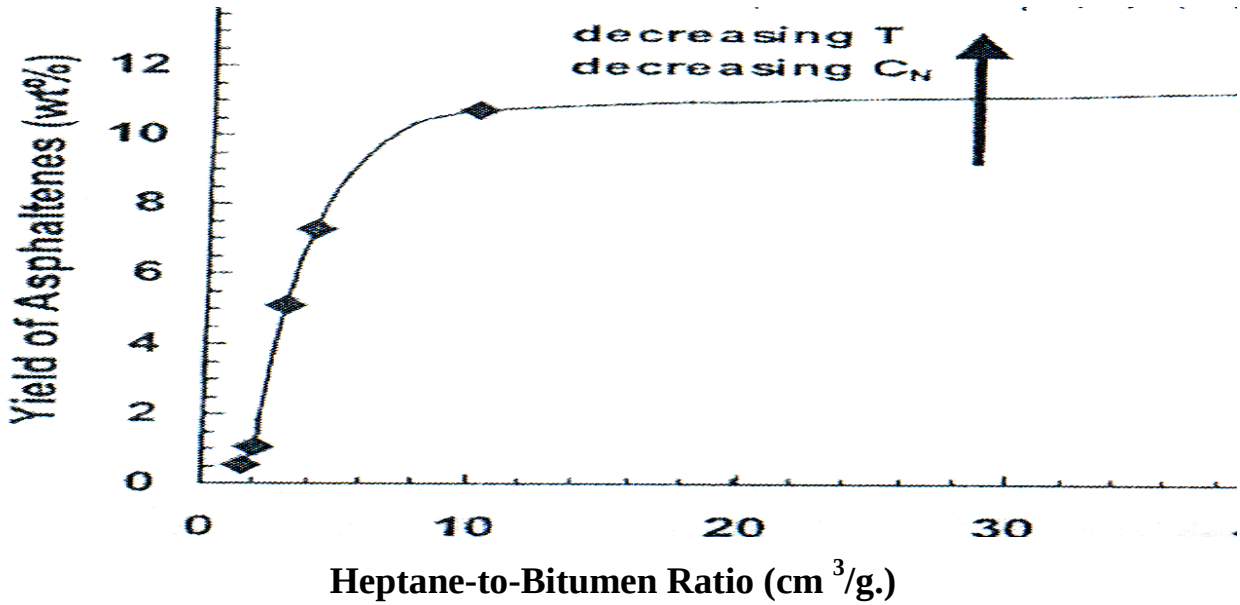

Figure-3: Effect of Solvent to Bitumen Ratio on the Yield of Asphaltenes

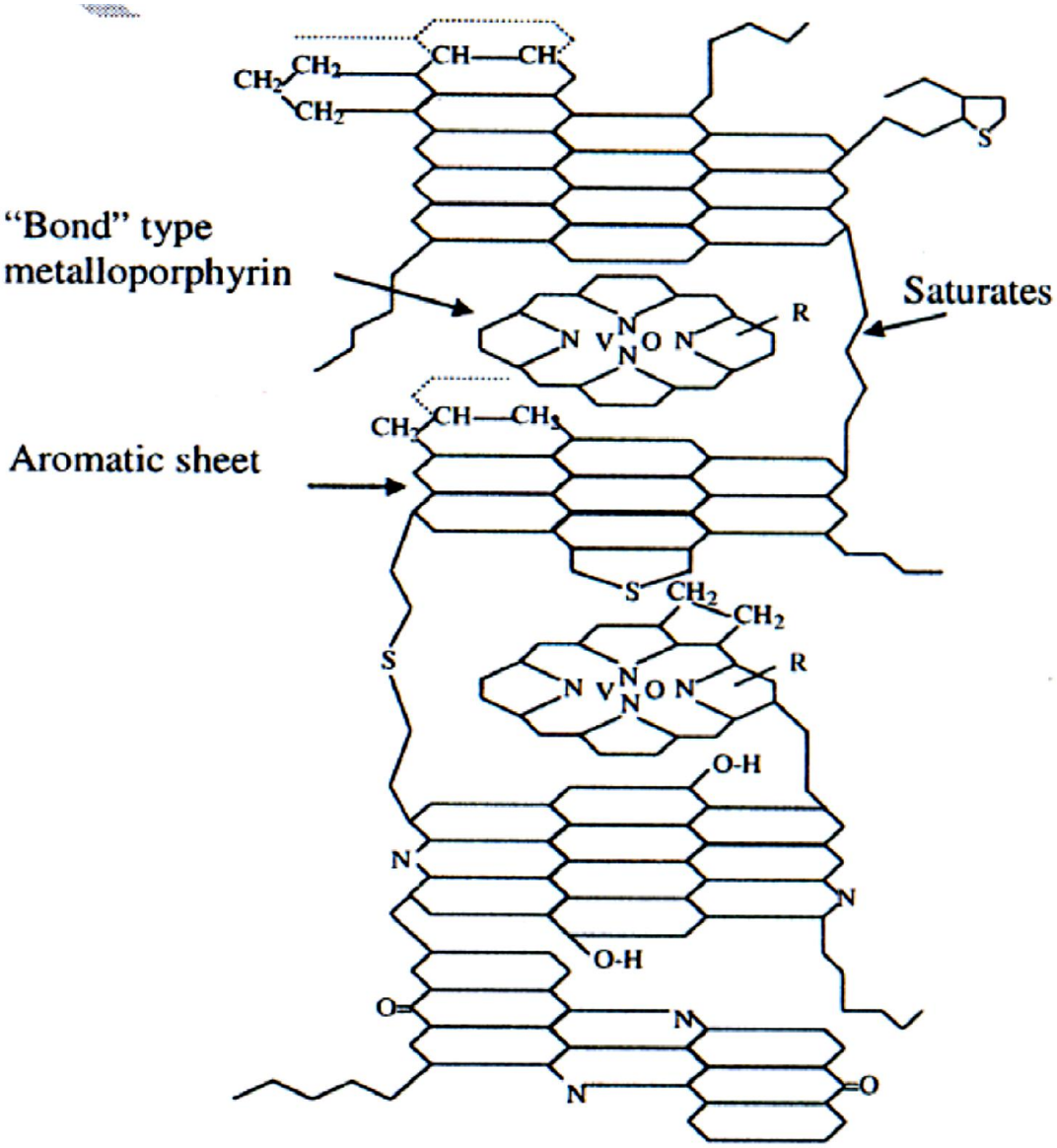

Figure-4: Hypothetical Asphaltene Molecule and its Interaction with the Metaloporfphyrins.

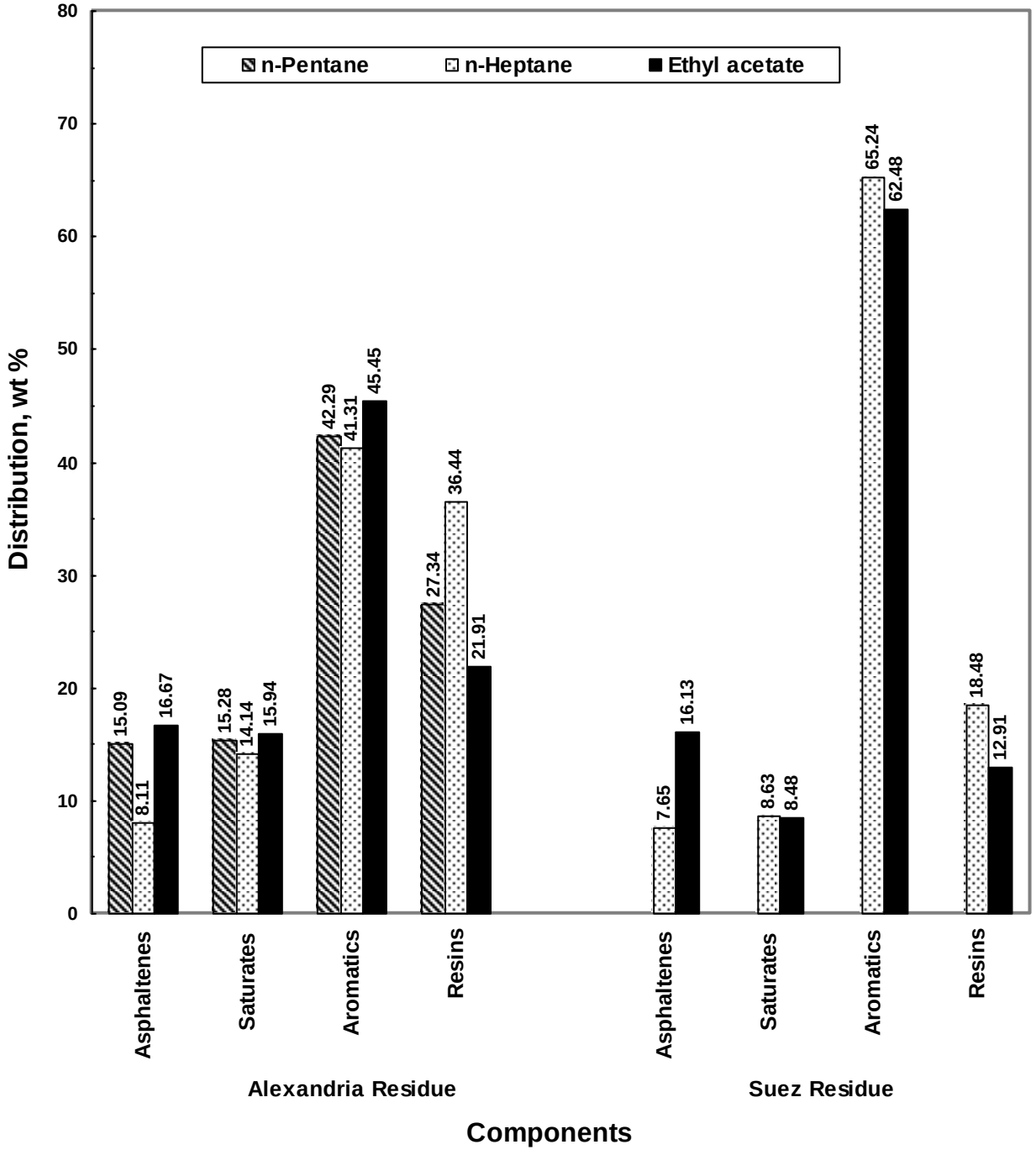

Figure-5. Distribution of the Saturates, Aromatics, Resins and Asphaltenes (SARA) in the Studied Vacuum Residues.

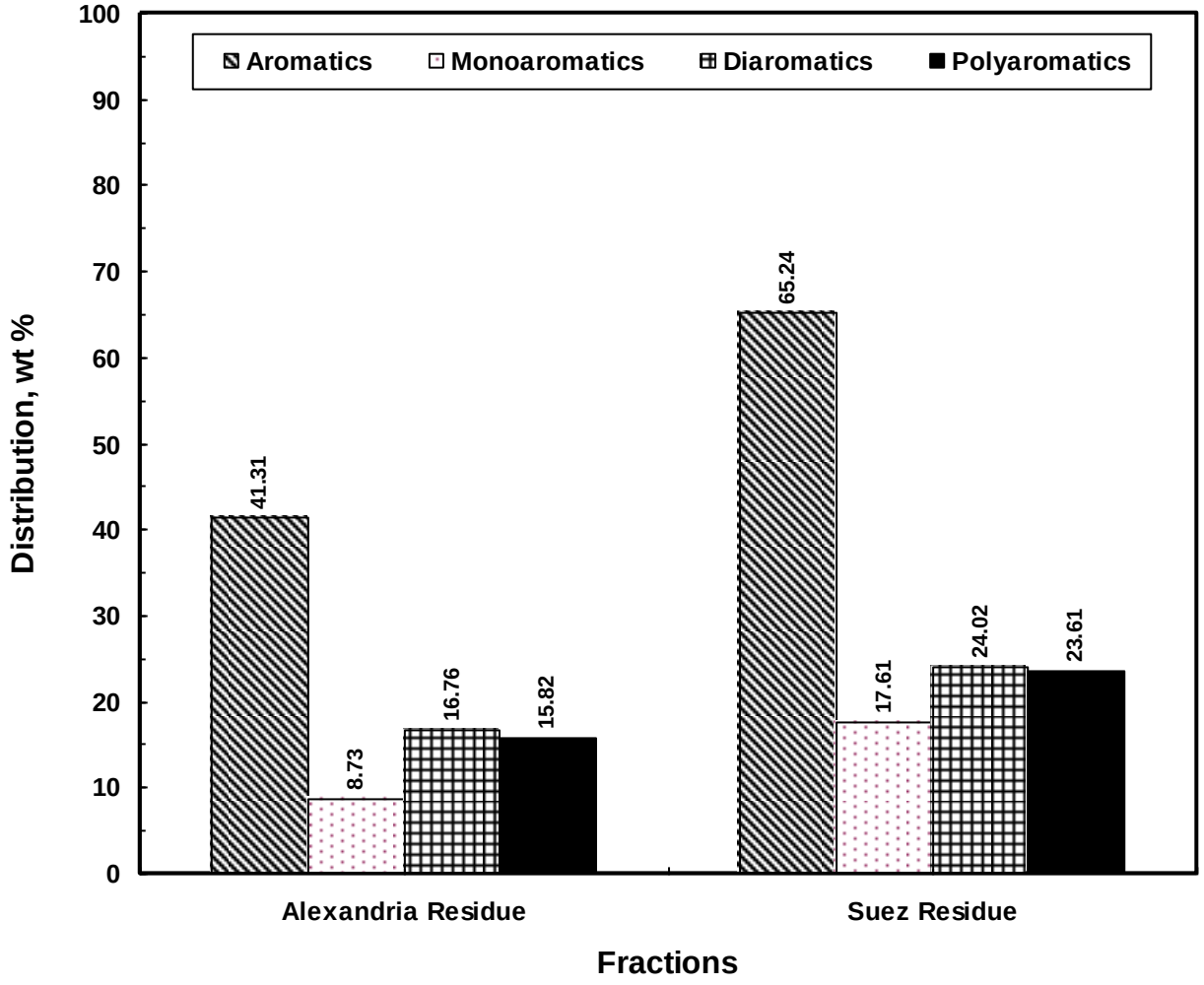

Figure-6. Distribution of the Aromatics, Mono, Di- and Poly-Aromatics In the Studied Vacuum Residues.

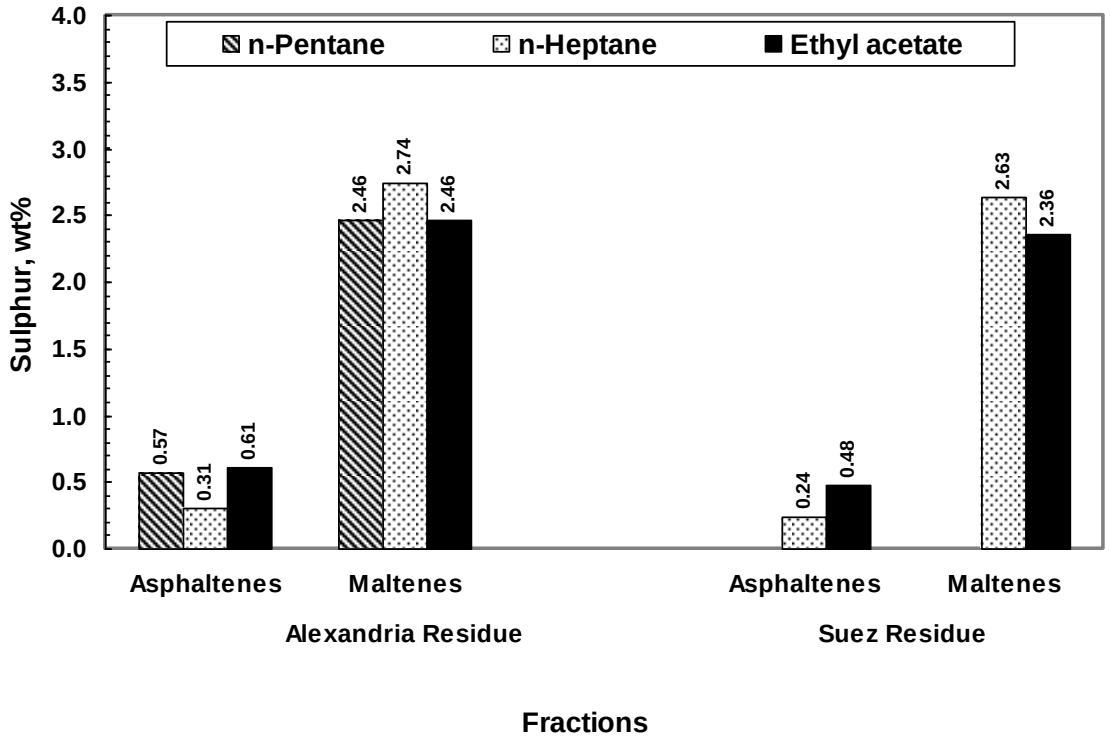

Figure-7: Distribution of the Sulphur in the Asphaltenes and Maltenes in the Studied Vacuum Residues.

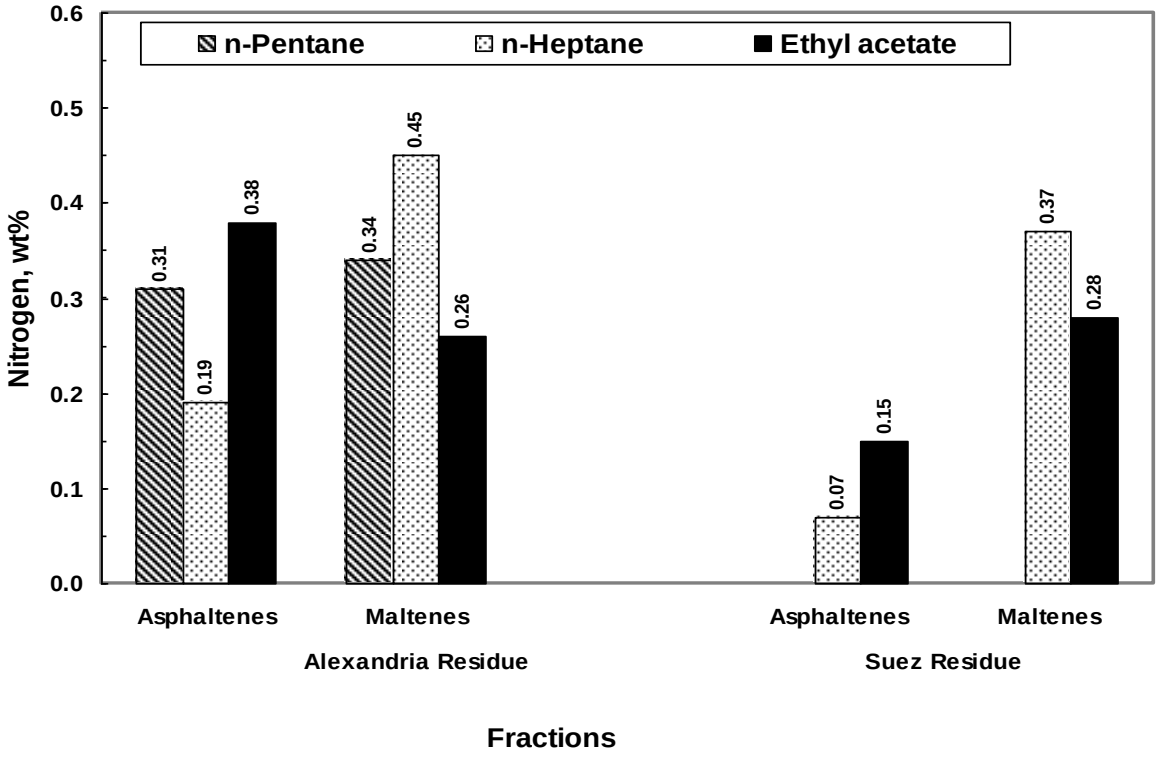

Figure-8: Distribution of the Nitrogen in the Asphaltenes and Maltenes in the Studied Vacuum Residues.

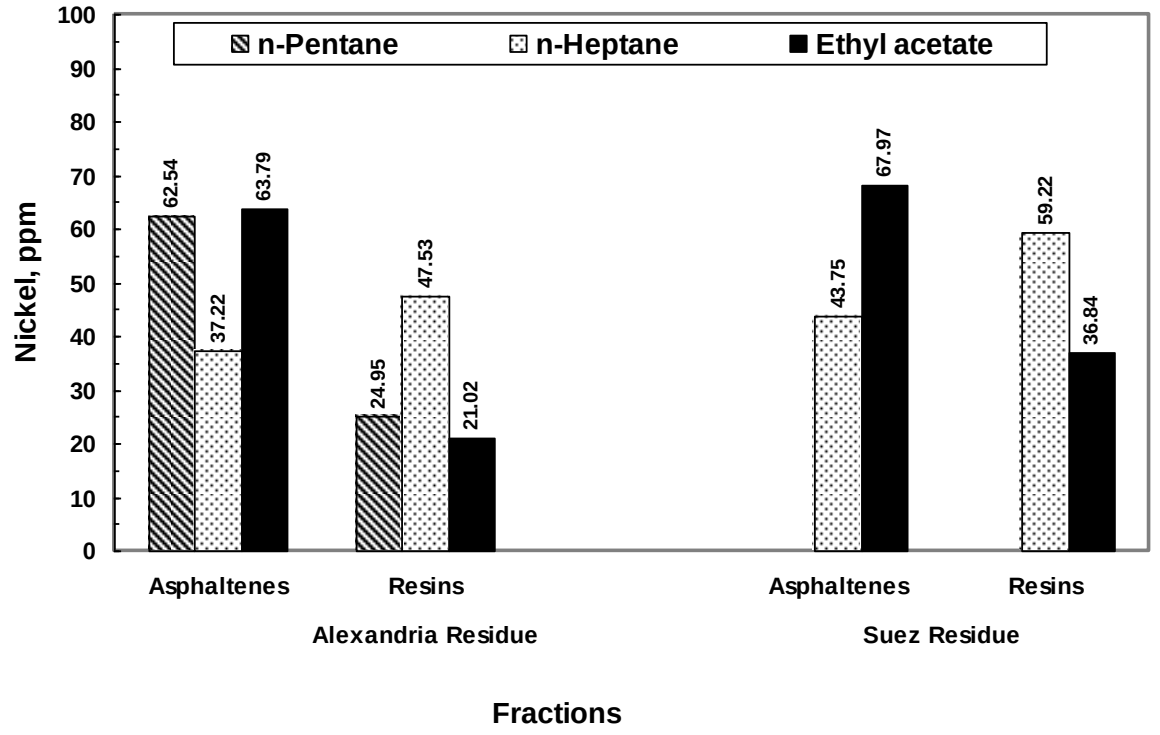

Figure-9: Distribution of the Nickel in the Asphaltenes and Rtesins in the Studied Vacuum Residues.

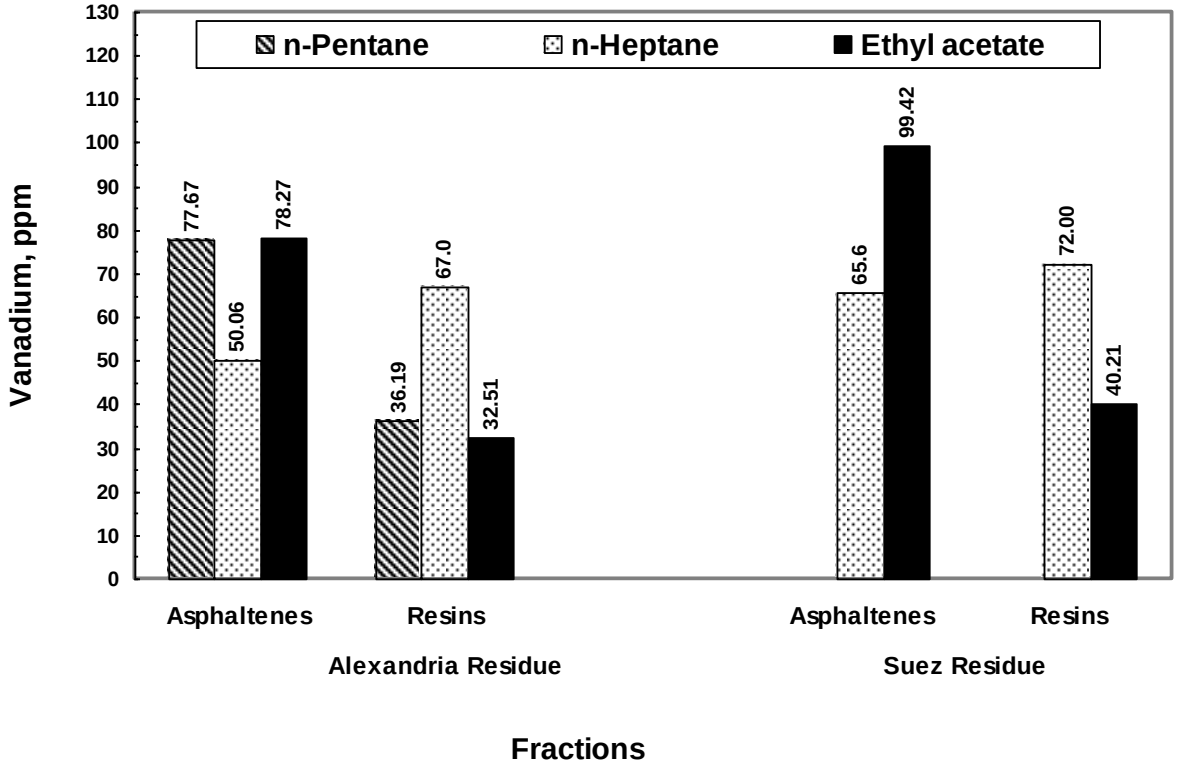

Figure-10: Distribution of the Vanadium in the Asphaltenes and Rtesins in the Studied Vacuum Residues.

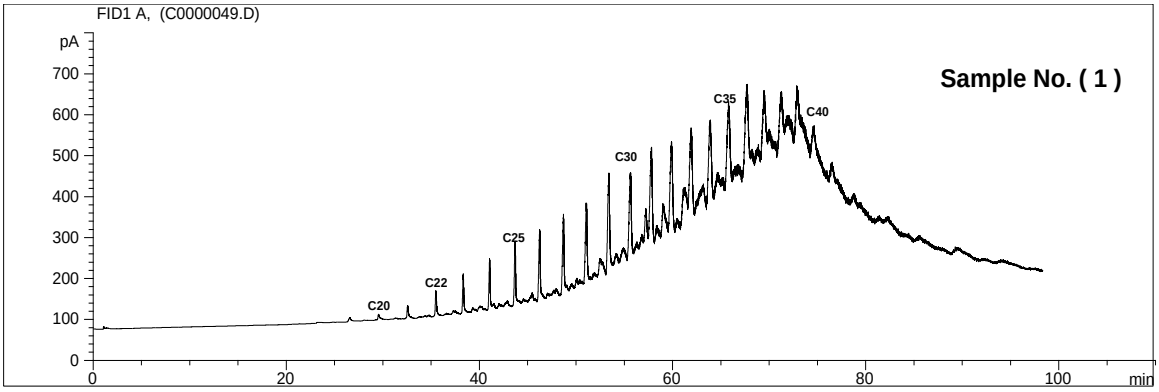

Figure-11:Gas chromatogram of Saturates Separated from Alexandria Residue Using n-Pentane

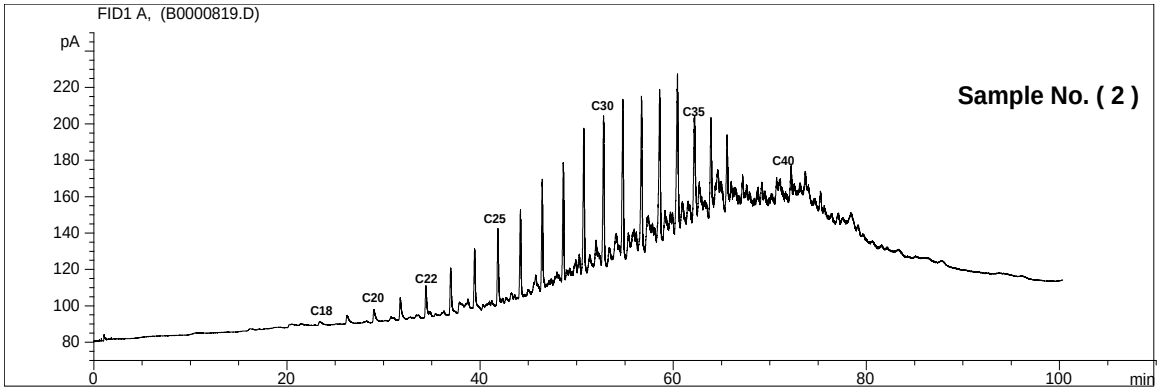

Figure-12:Gas chromatogram of Saturates Separated from Alexandria Residue Using n-Heptane

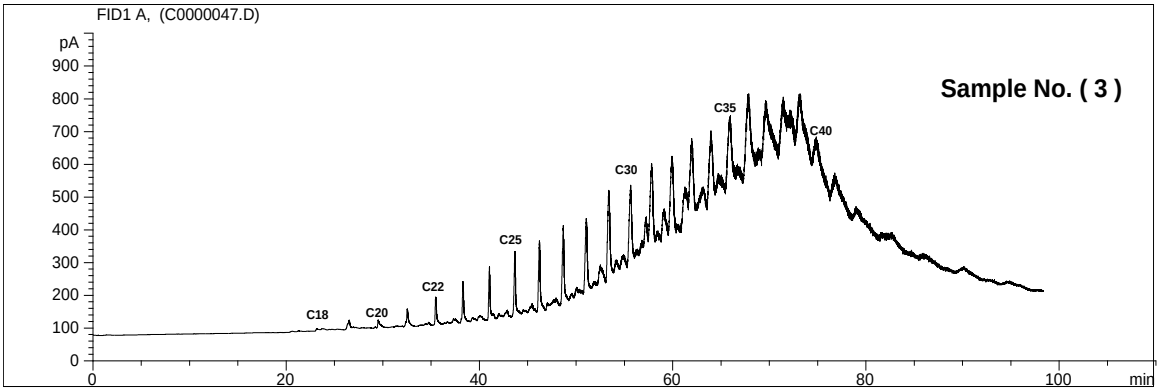

Figure-13:Gas chromatogram of Saturates Separated from Alexandria Residue Using Ethyl Acetate

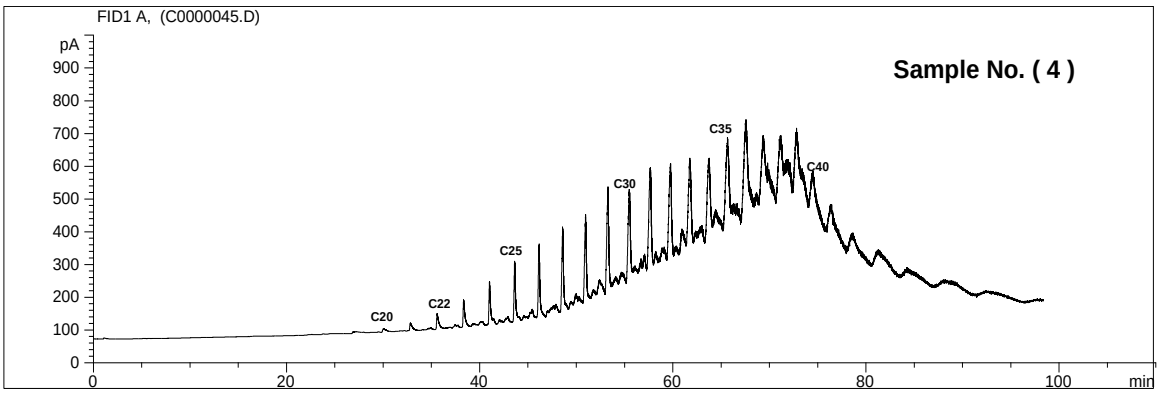

Figure-14:Gas chromatogram of Saturates Separated from Suez Residue Using n- Heptane

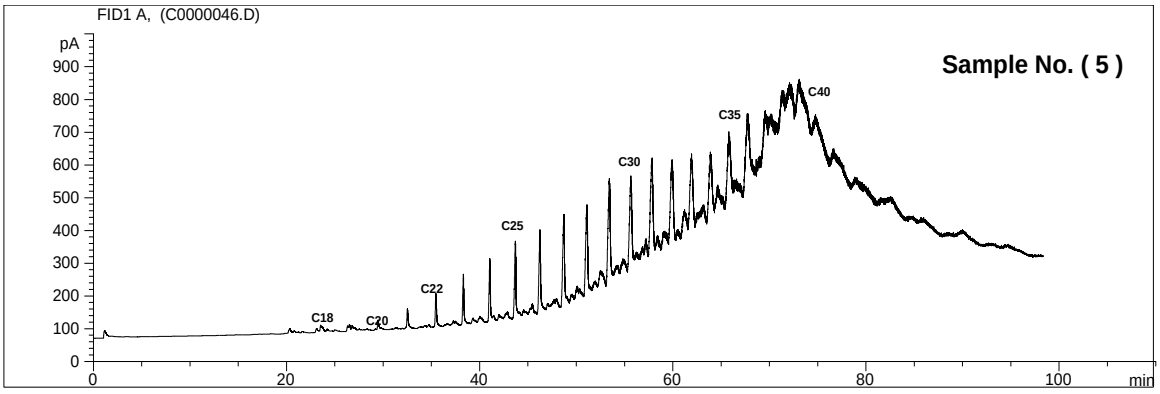

Figure-15:Gas chromatogram of Saturates Separated from Suez Residue Using Ethyl Acetate

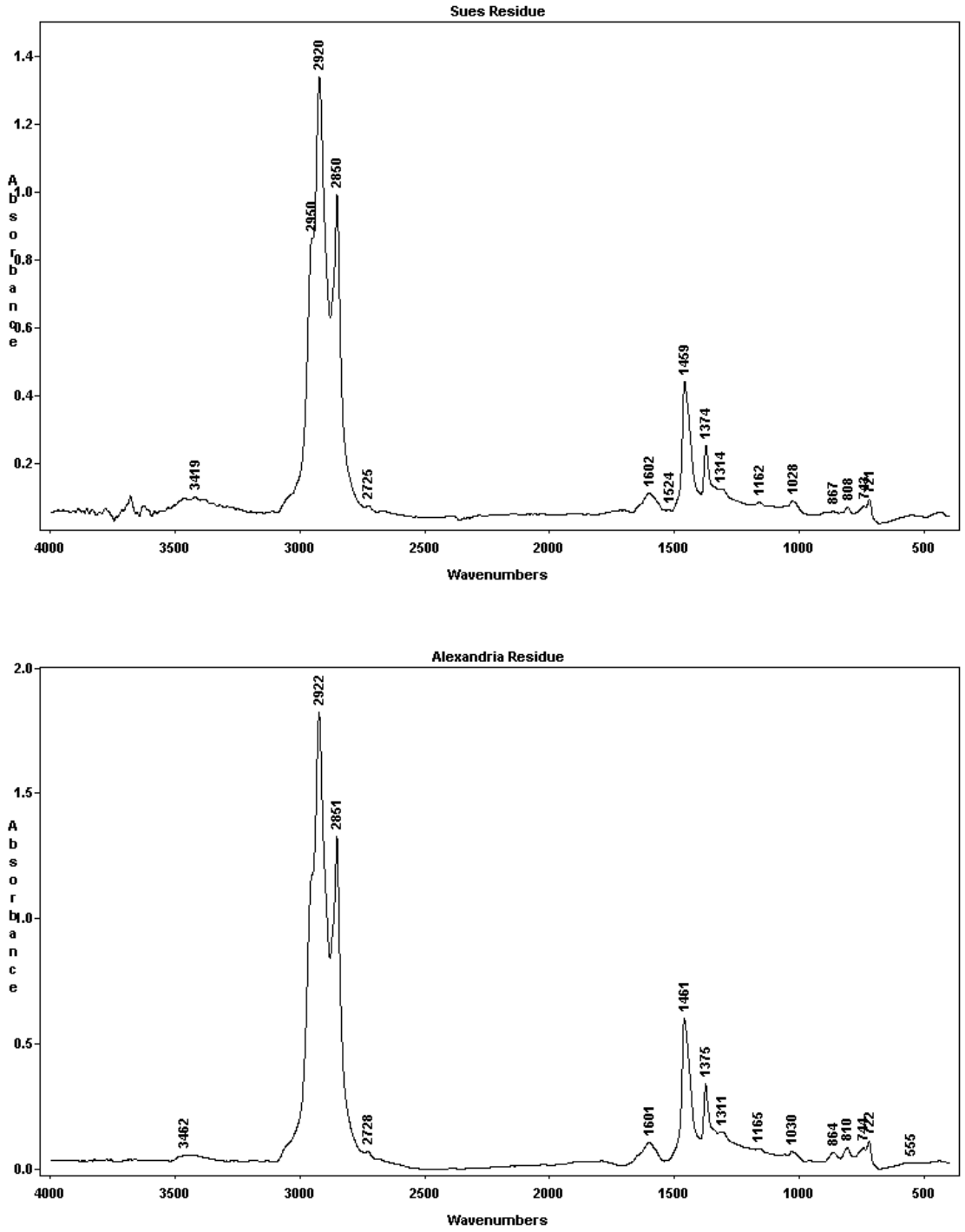

Figure-16: Infrared Spectra of the Studied Vacuum Residues.

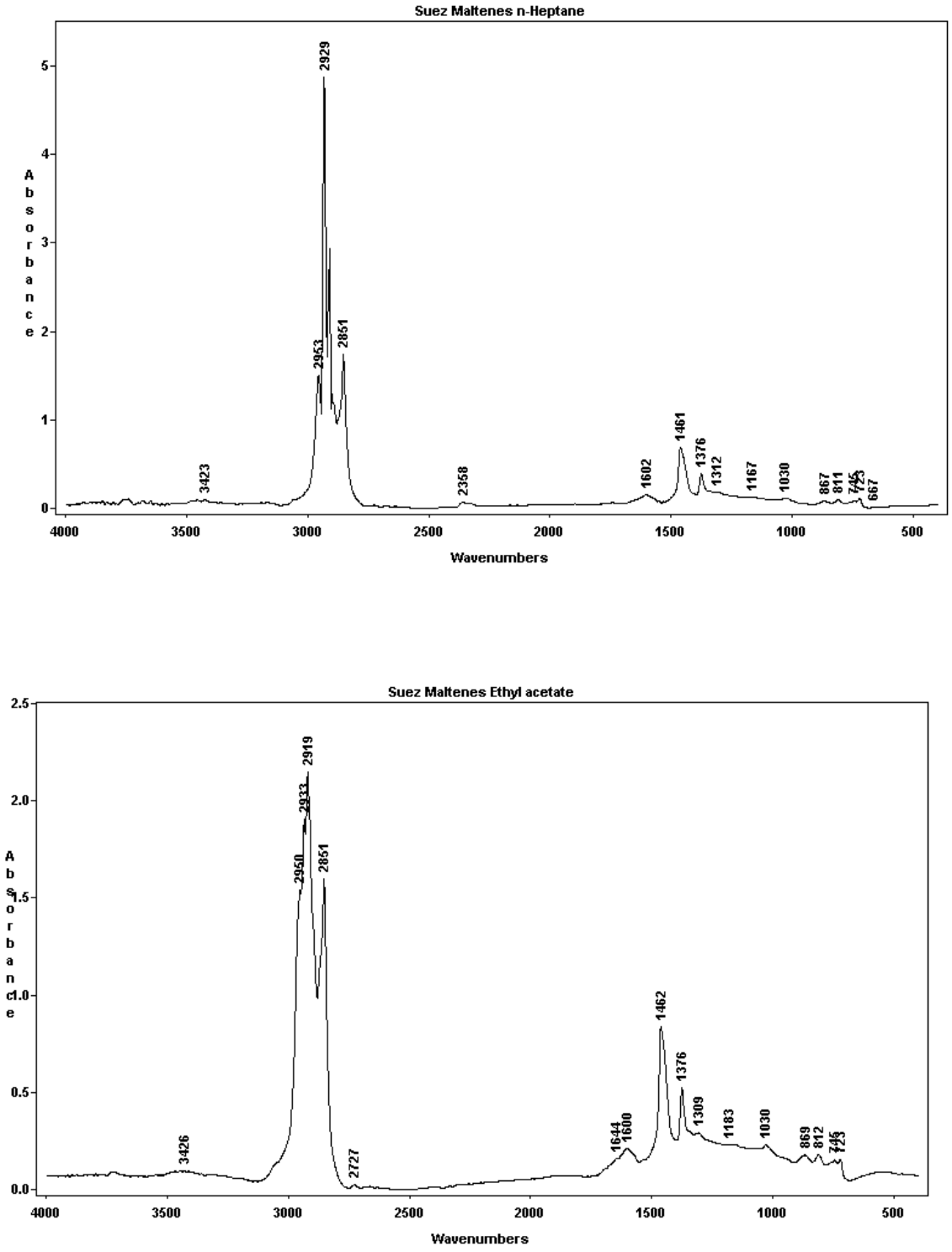

Figure-17: Infrared Spectra of the Suez Maltenes as Separated By *n*-Heptane and Ethyl Acetate Solvents.

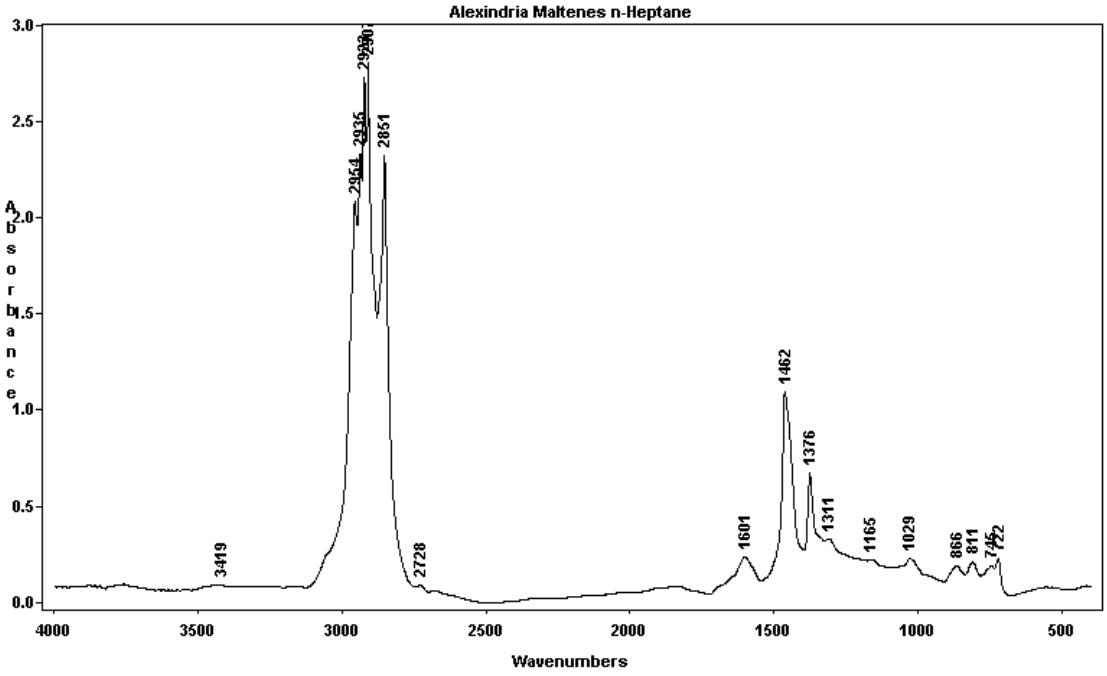

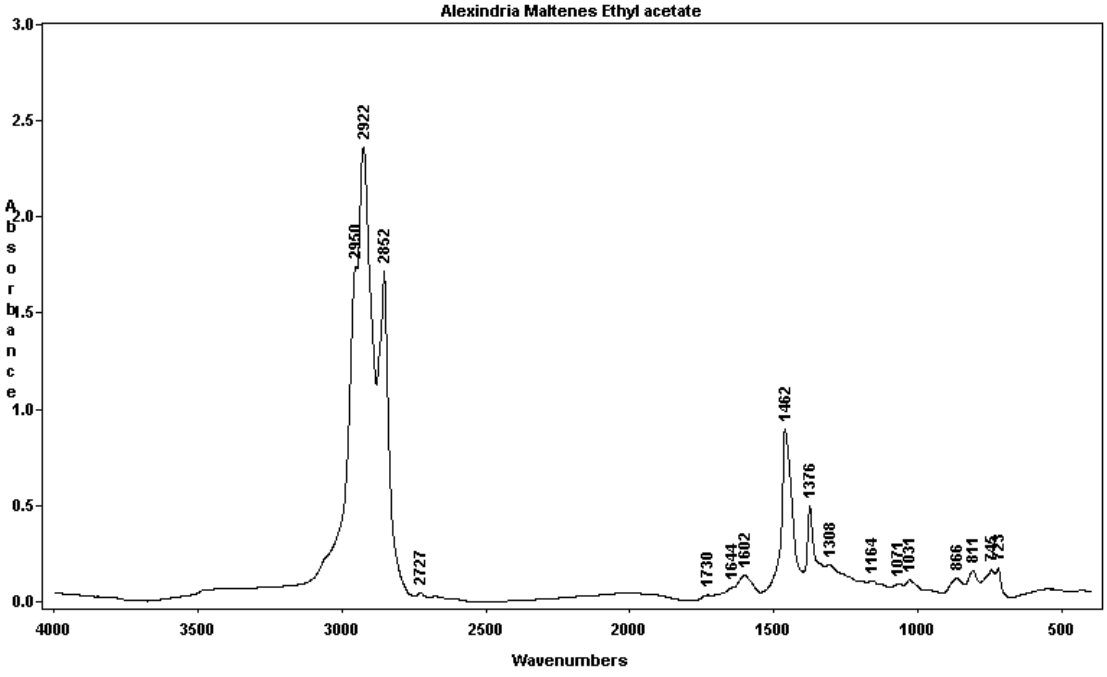

Figure-18: Infrared Spectra of the Alexandria Maltenes as Separated By *n*-Heptane and Ethyl Acetate Solvents.

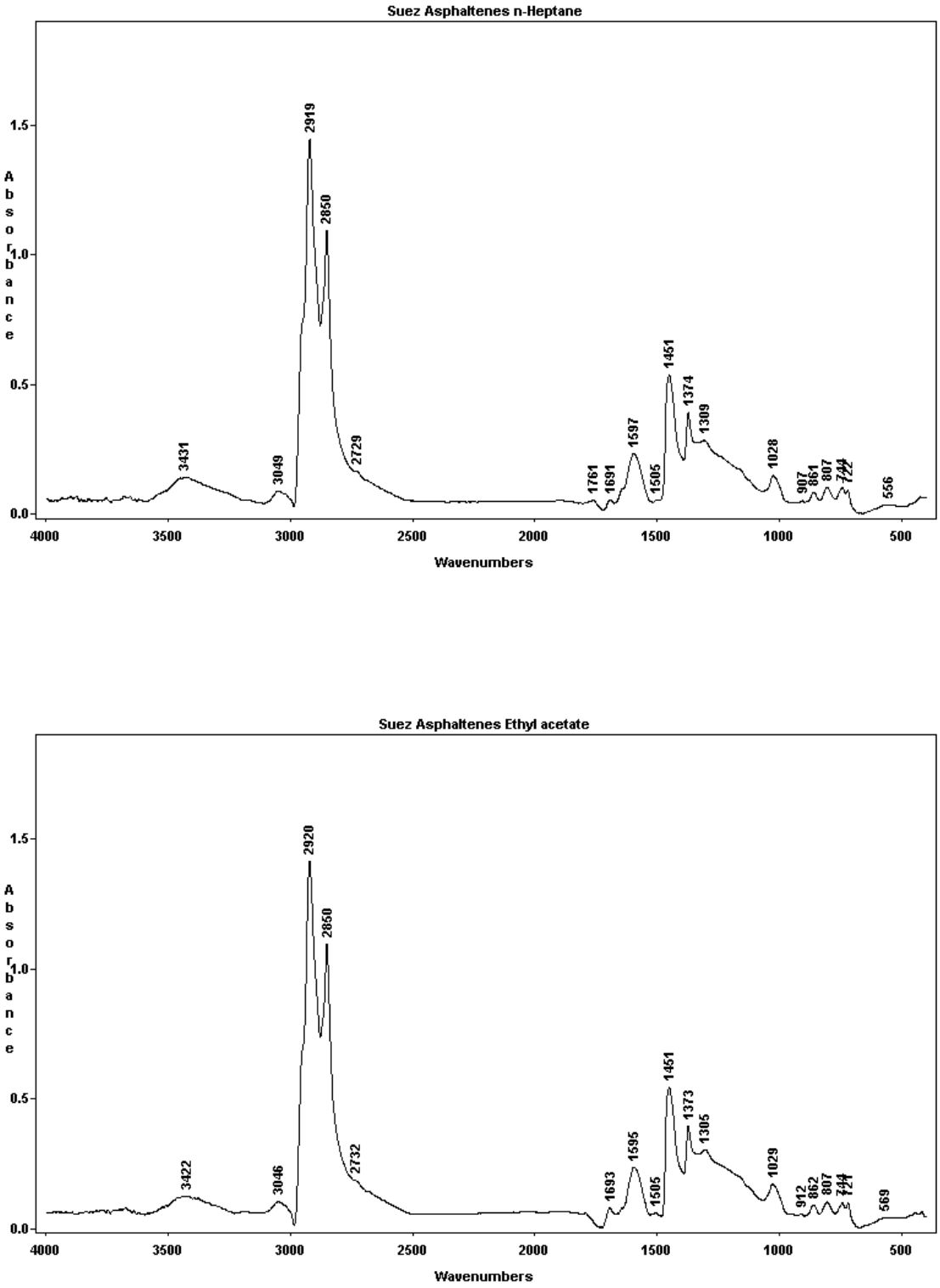

Figure-19: Infrared Spectra of the Suez Asphaltenes as Separated By *n*-Heptane and Ethyl Acetate Solvents.

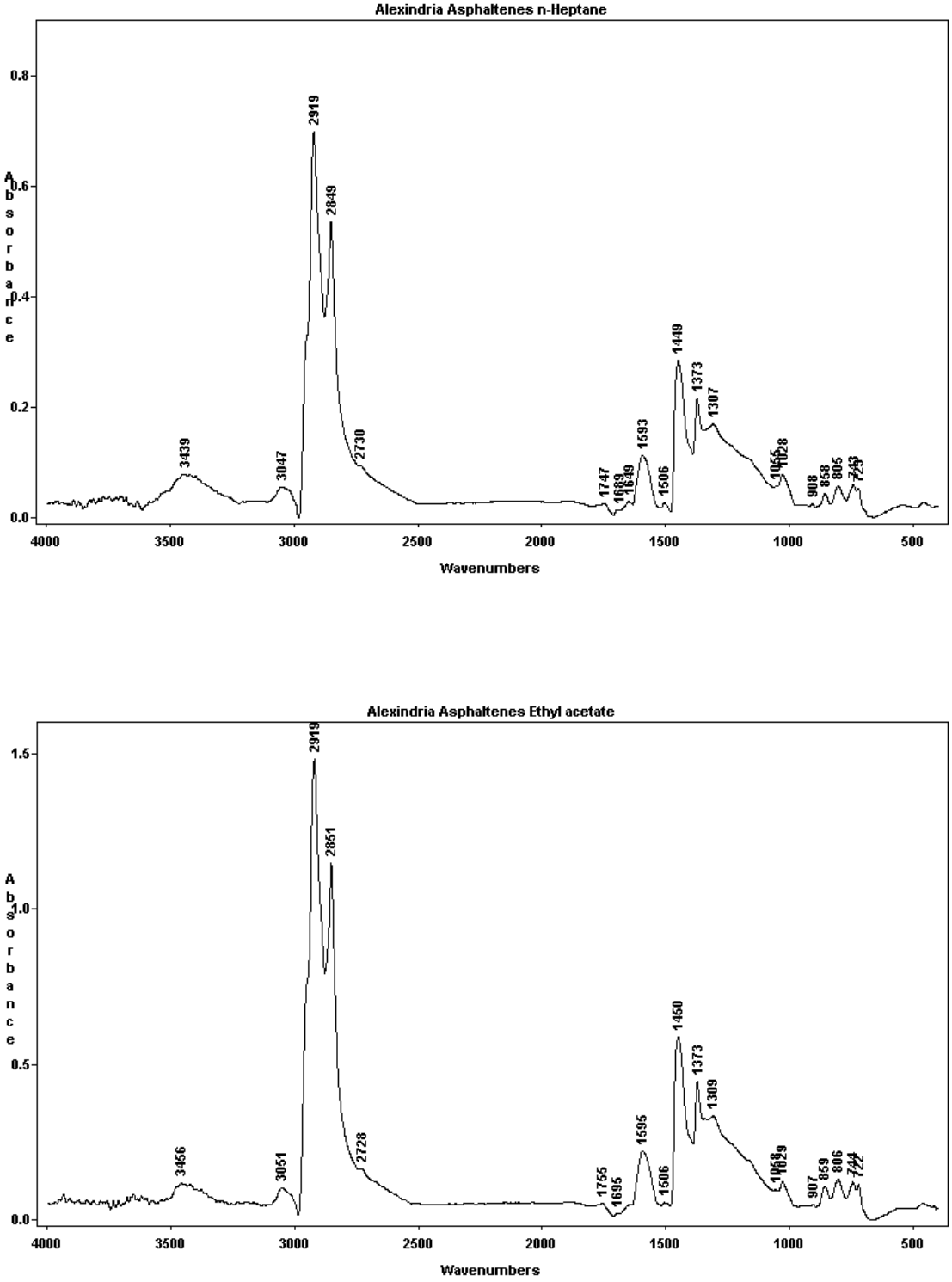

Figure-20: Infrared Spectra of the Alexandria Asphaltenes as Separated By *n*-Heptane and Ethyl Acetate Solvents.

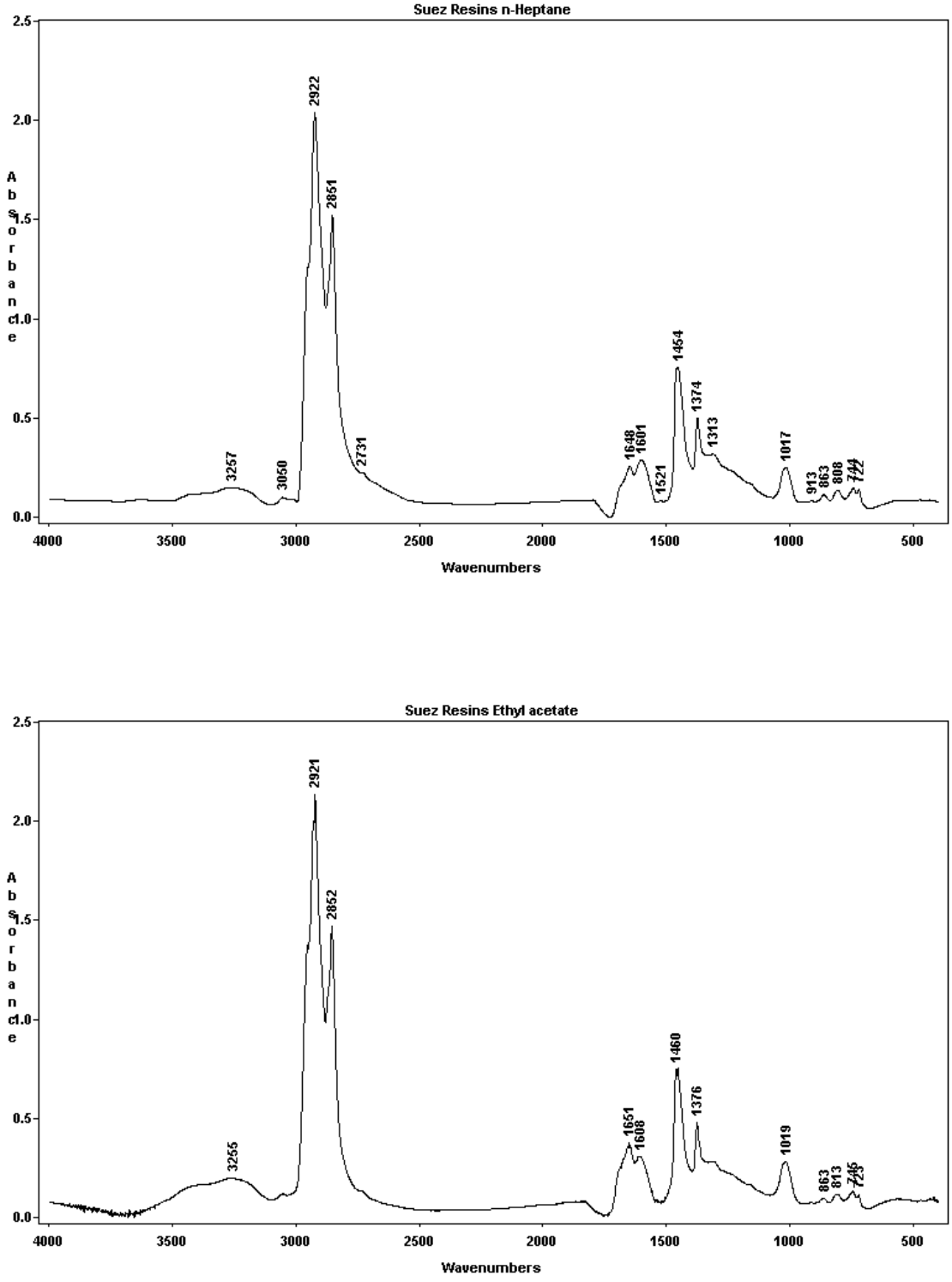

Figure-21: Infrared Spectra of the Suez Resins as Separated By *n*-Heptane and Ethyl Acetate Solvents.

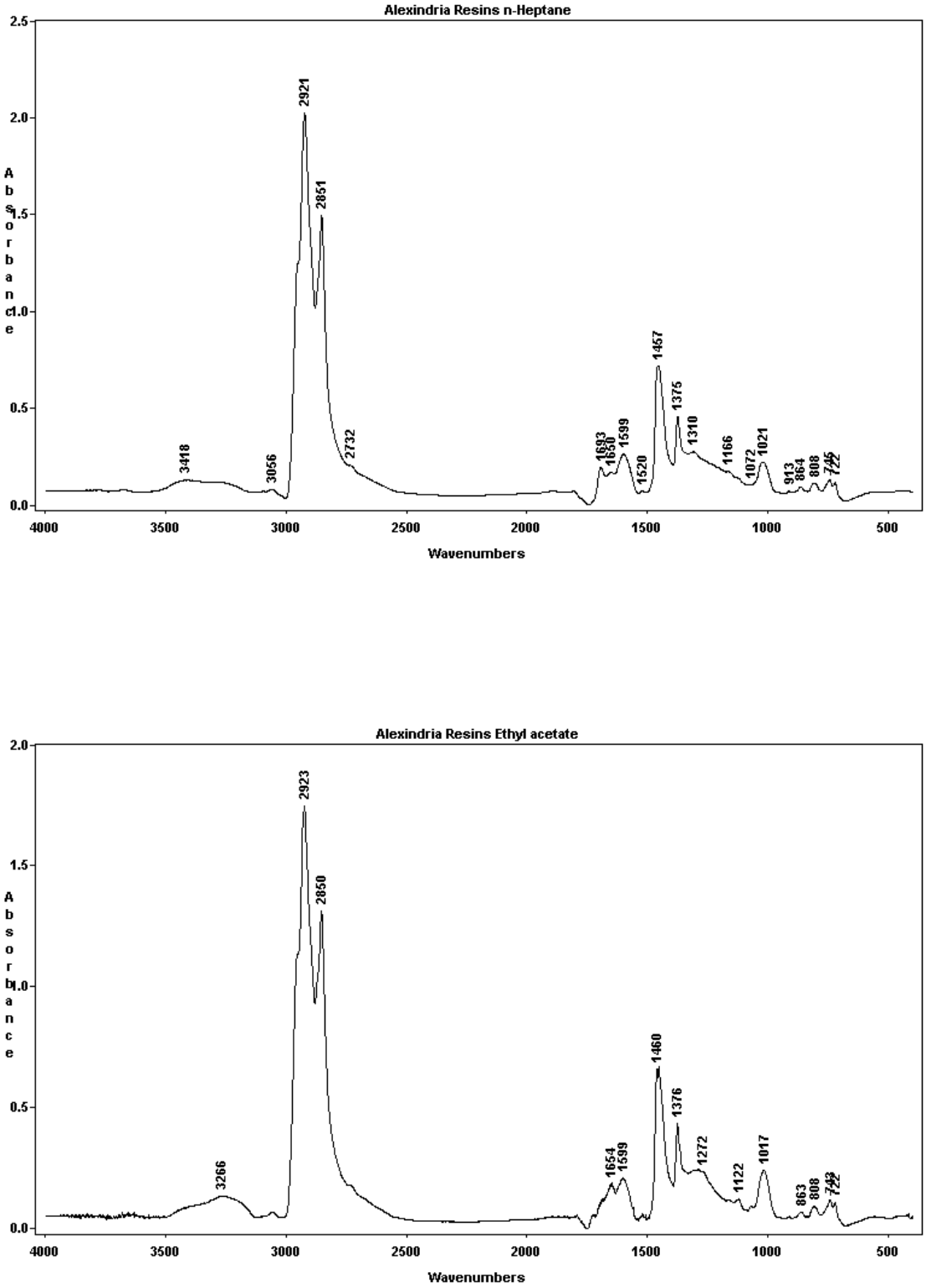

Figure-22: Infrared Spectra of the Alexandria Resins as Separated By *n*-Heptane and Ethyl Acetate Solvents.

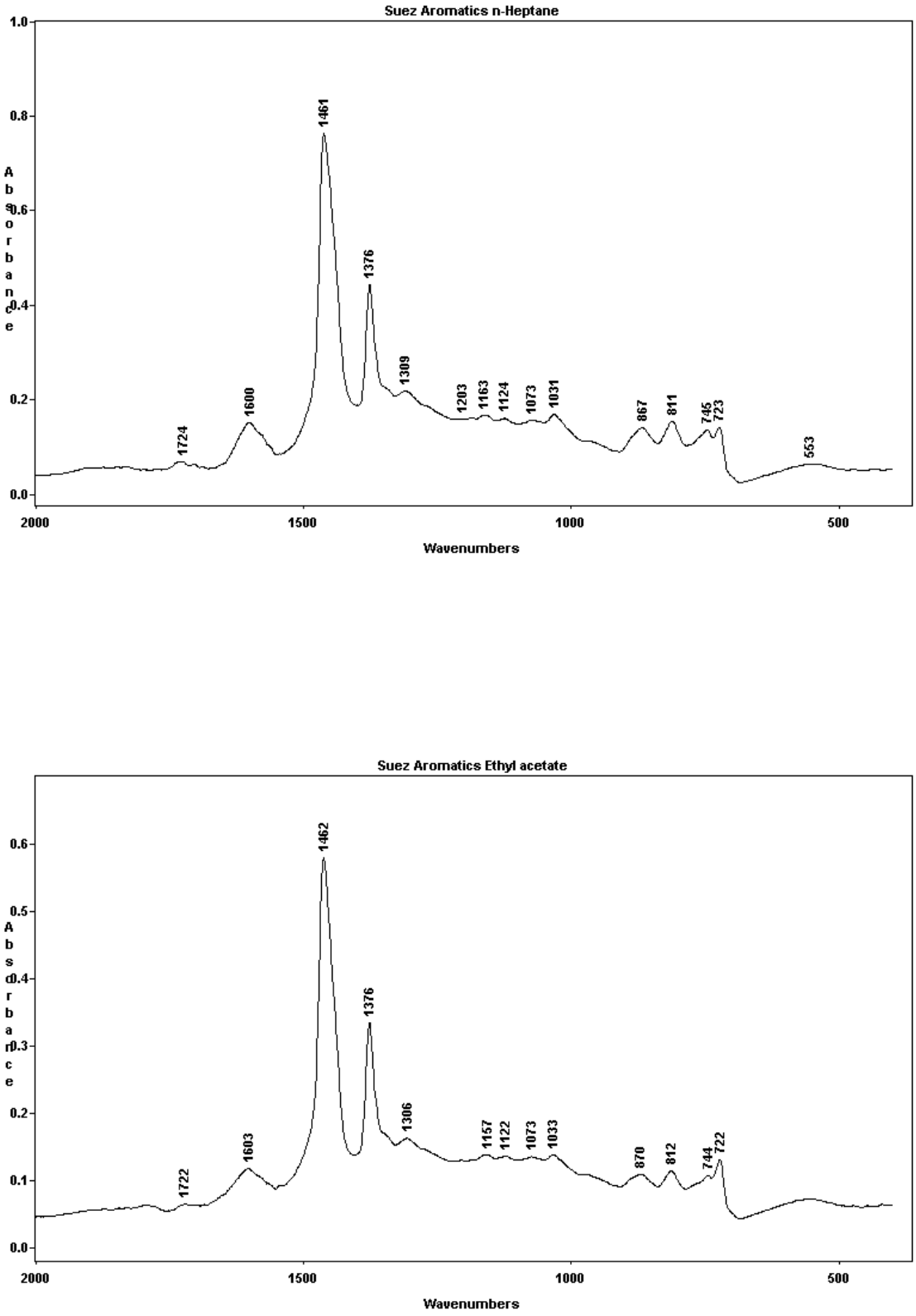

Figure-23: Infrared Spectra of the Suez Aromatics as Separated By *n*-Heptane and Ethyl Acetate Solvents.

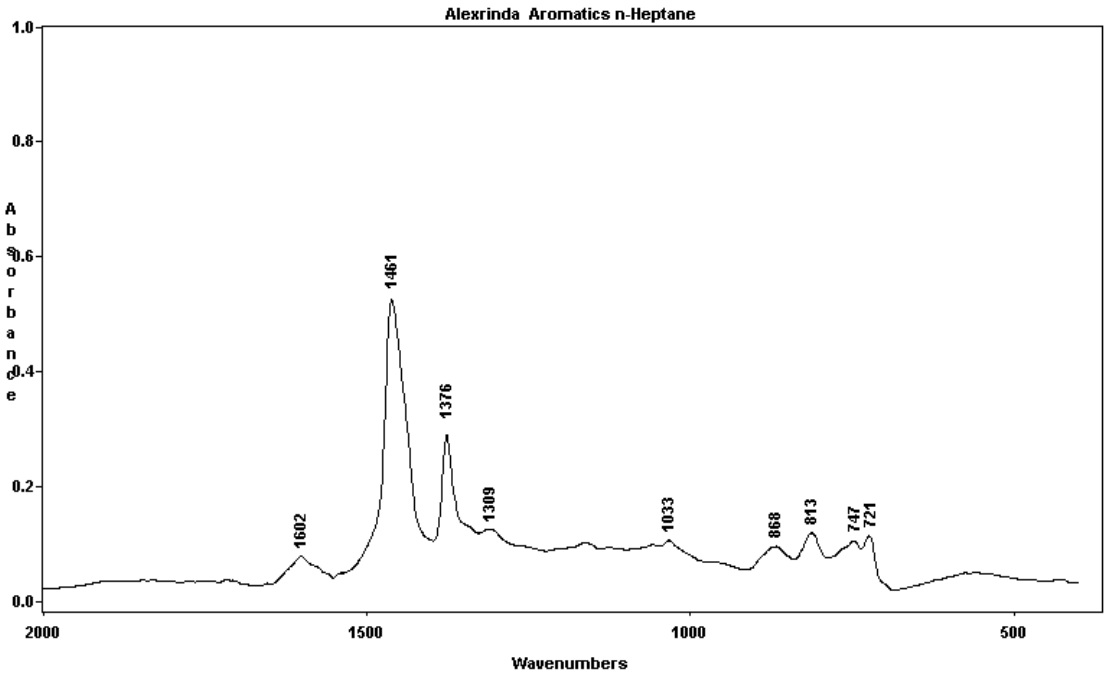

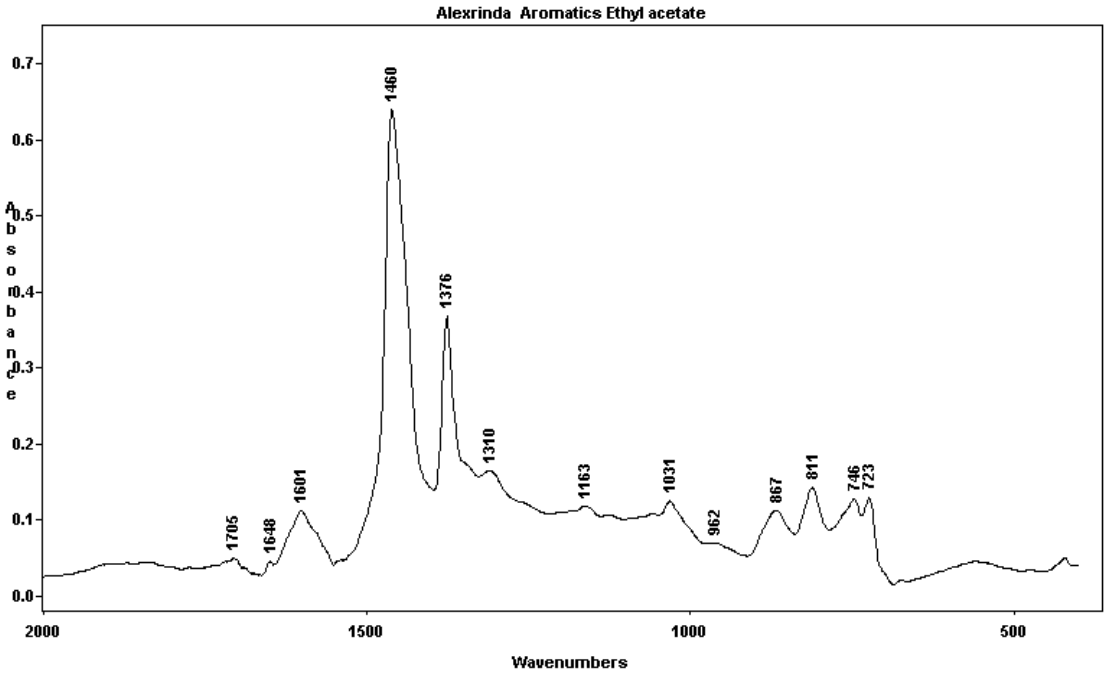

Figure-24: Infrared Spectra of the Alexandria Aromatics as Separated By *n*-Heptane and Ethyl Acetate Solvents.

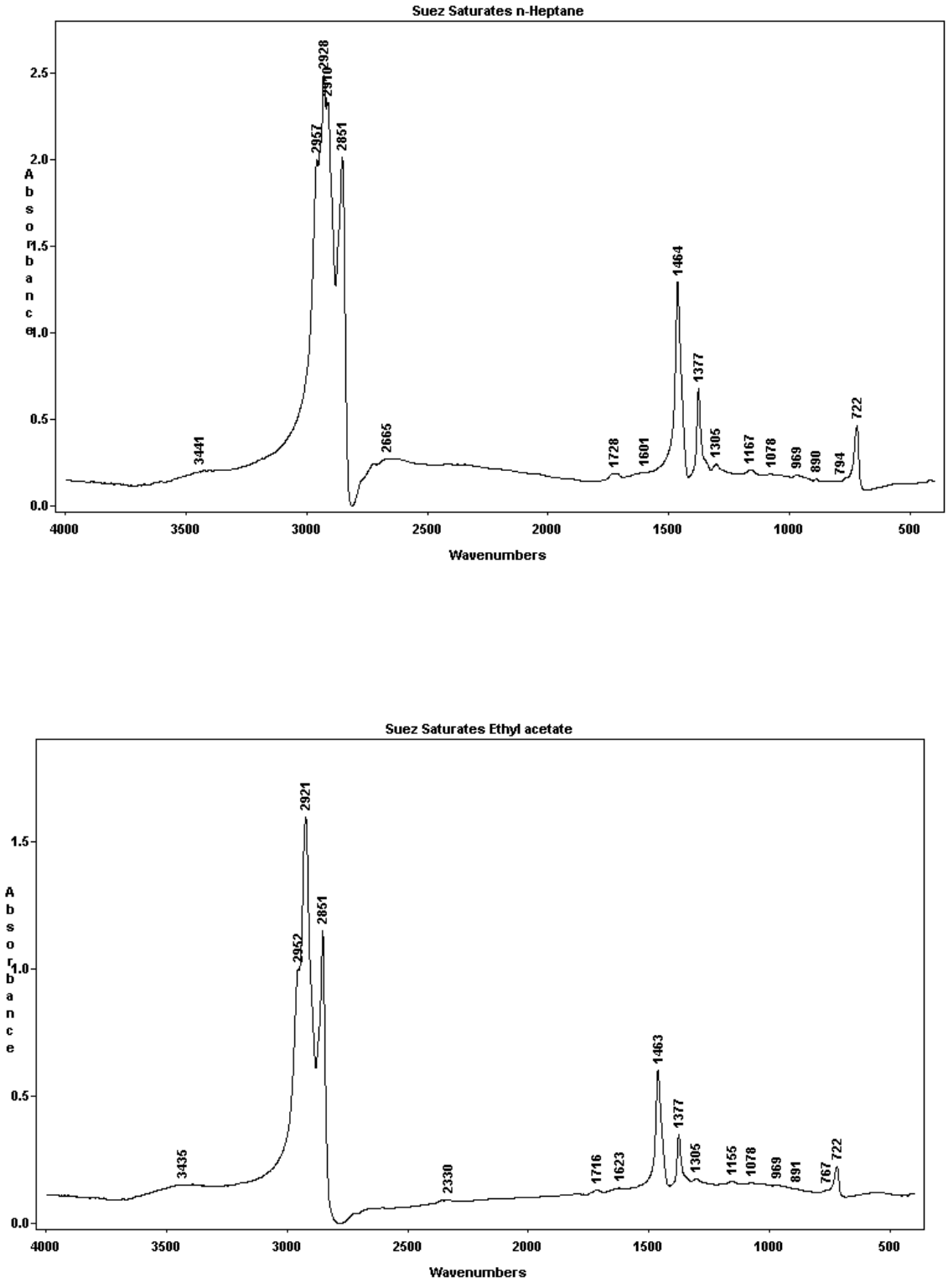

Figure-25: Infrared Spectra of the Suez Saturates as Separated By *n*-Heptane and Ethyl Acetate Solvents.

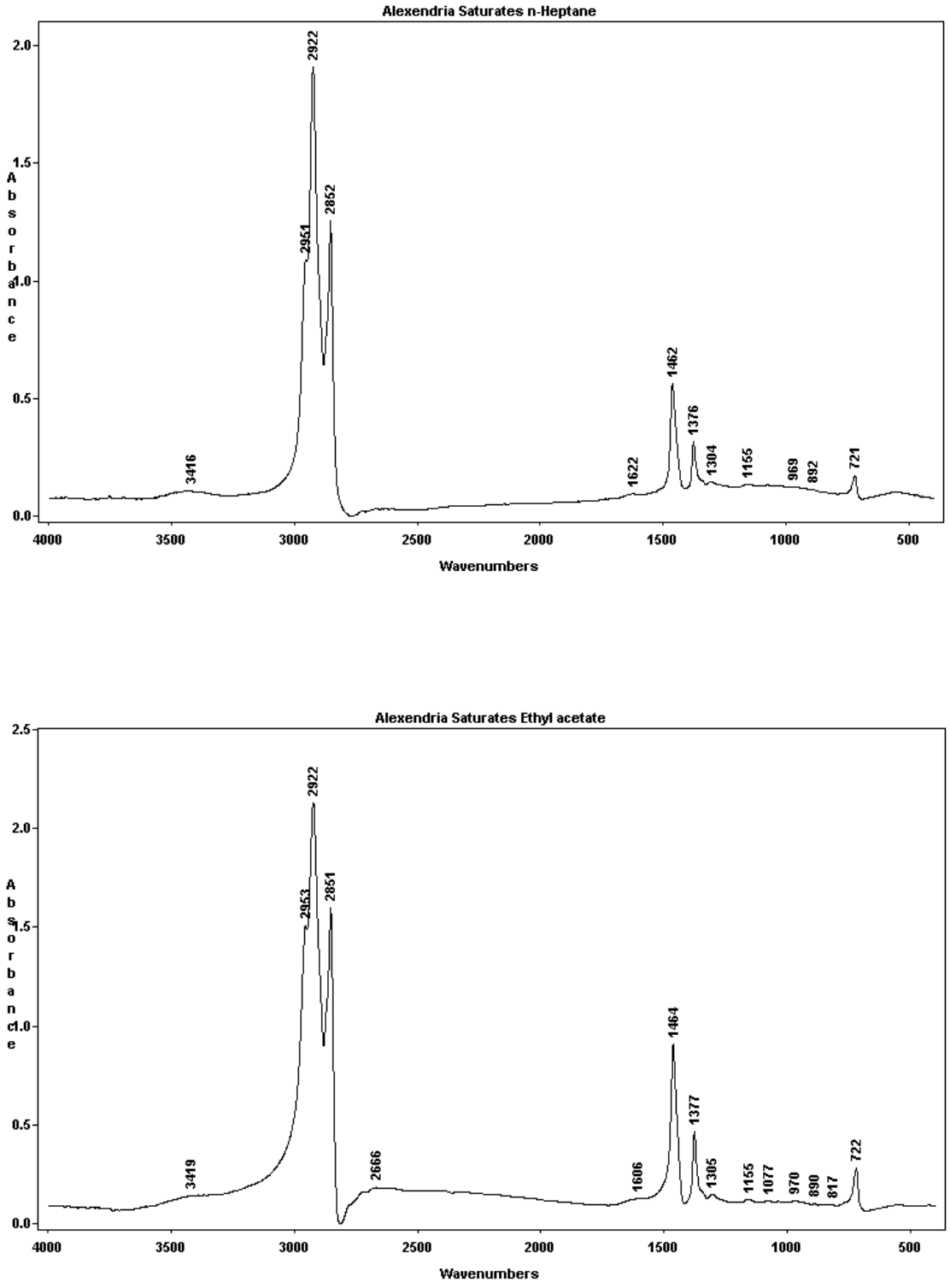

Figure-26: Infrared Spectra of the Alexandria Saturates as Separated By *n*-Heptane and Ethyl Acetate Solvents.

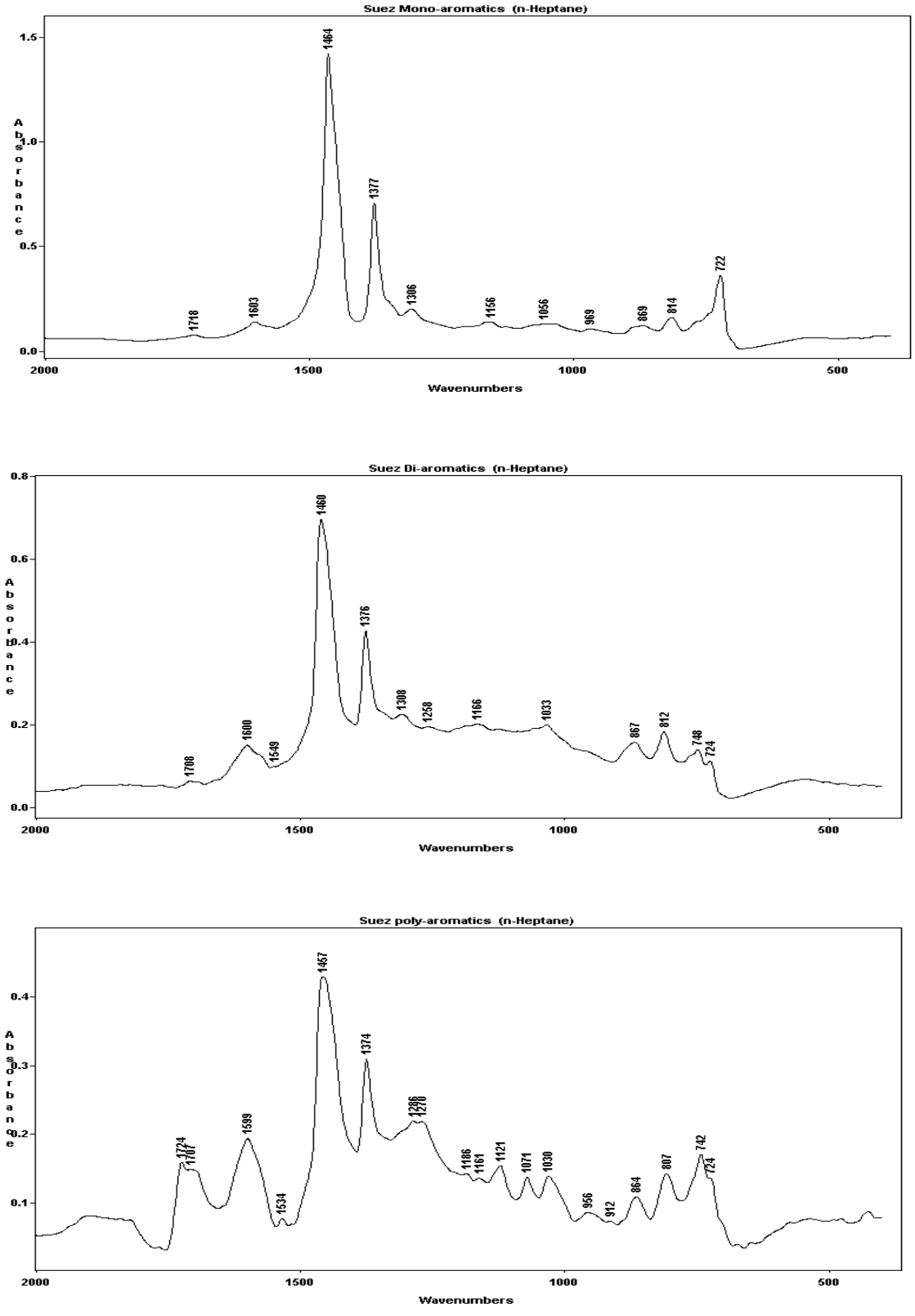

Figure-27:Infrared Spectra of the Suez Mono-, Di-, and Poly-Aromatics as Separated By *n*-Heptane Solvent.

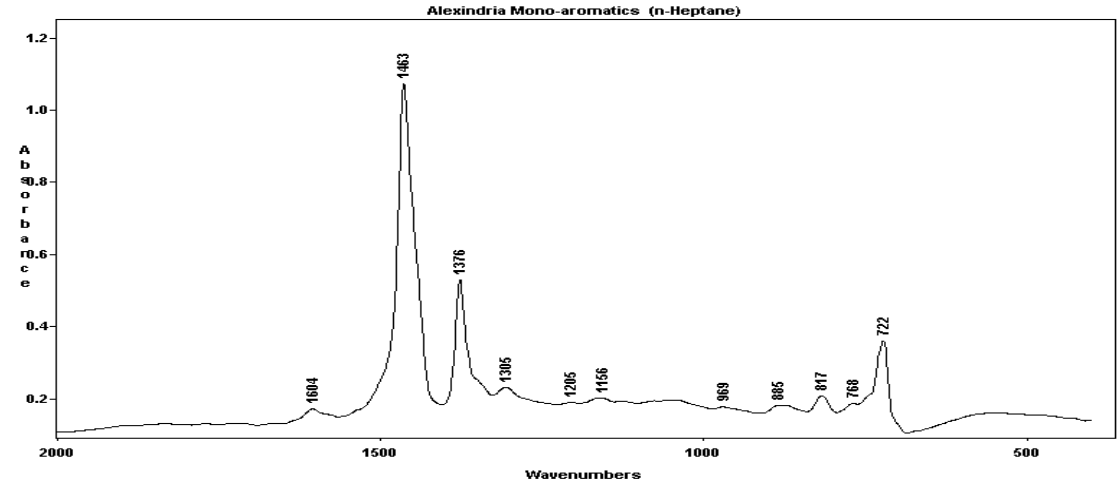

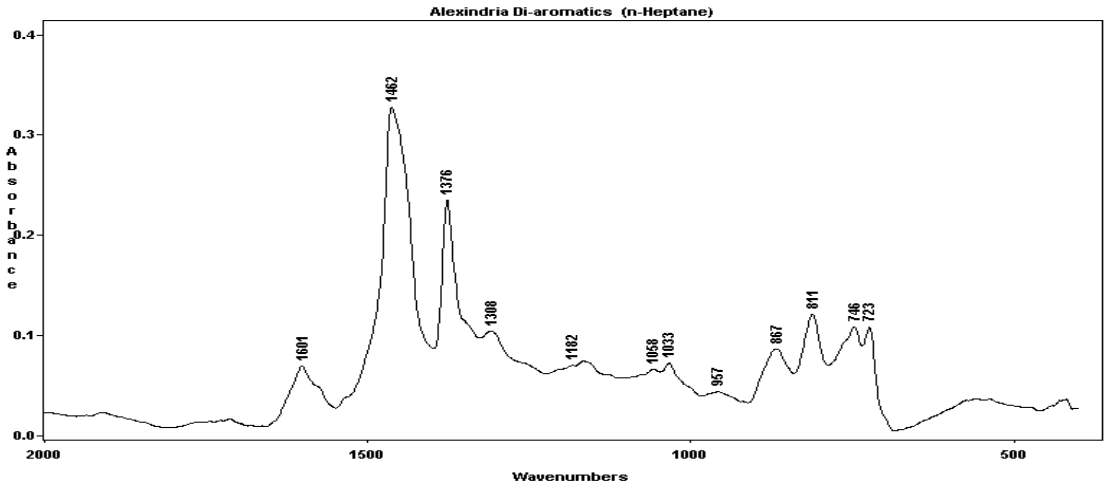

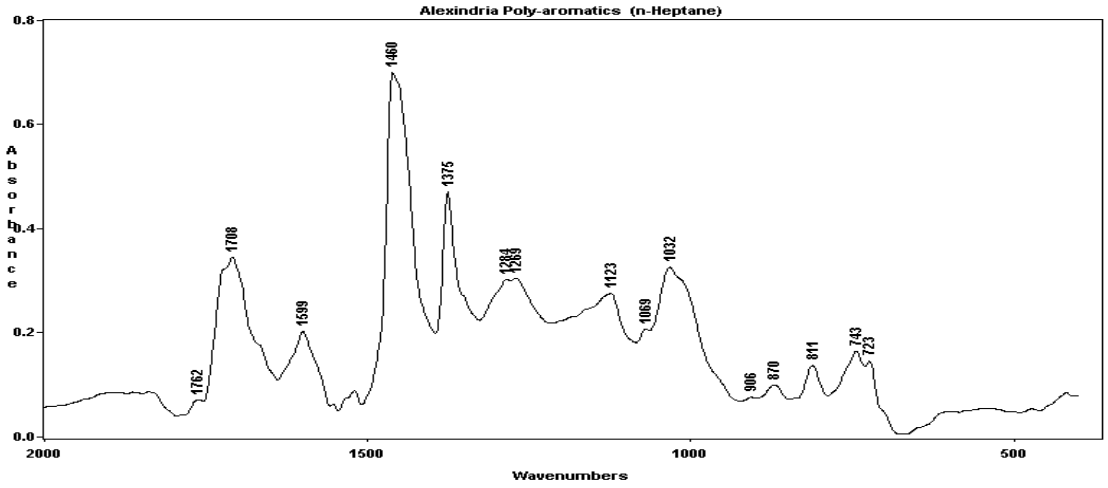

Figure-28:Infrared Spectra of the Alexandria Mono-, Di-, and Poly-Aromatics as Separated By *n*-Heptane Solvent.

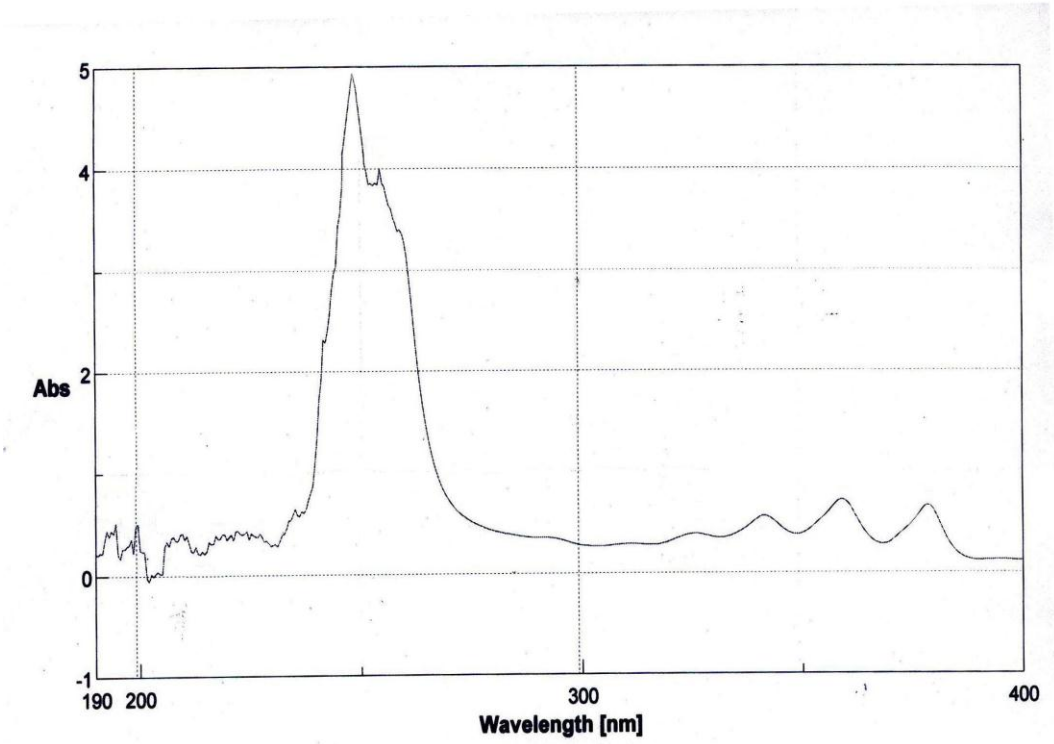

Suez Vacuum Residue

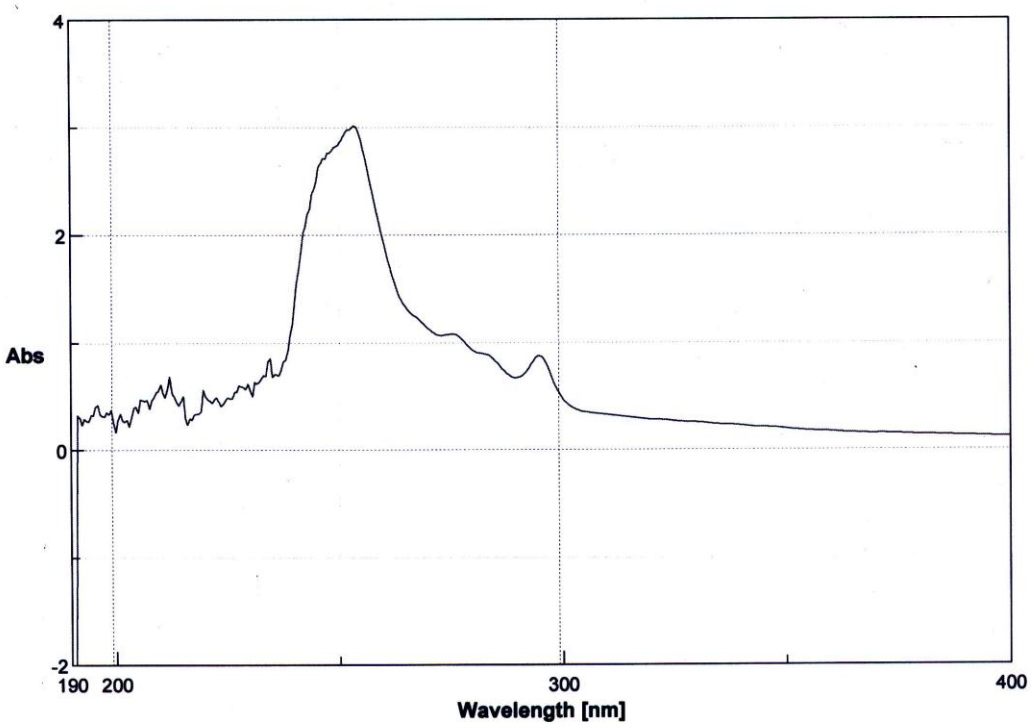

Alexandria Vacuum Residue

Figure-29: Ultraviolet Spectra of the Suez and Alexandria Vacuum Residues.

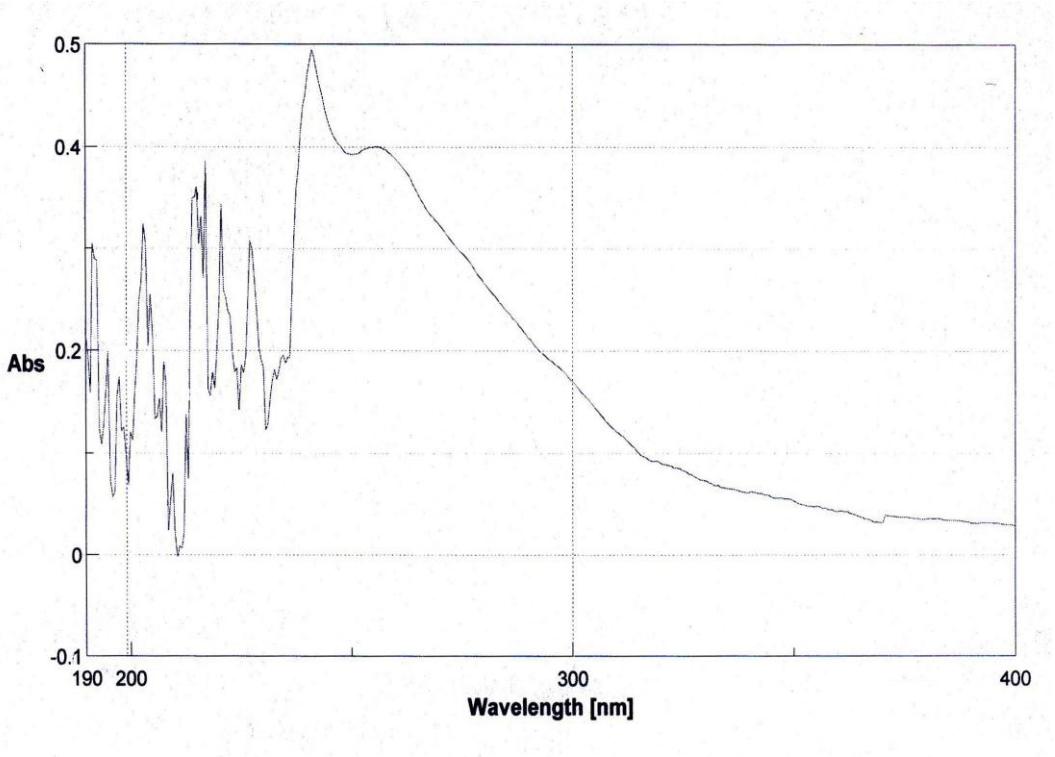

Suez *n*-Heptane Aromatics

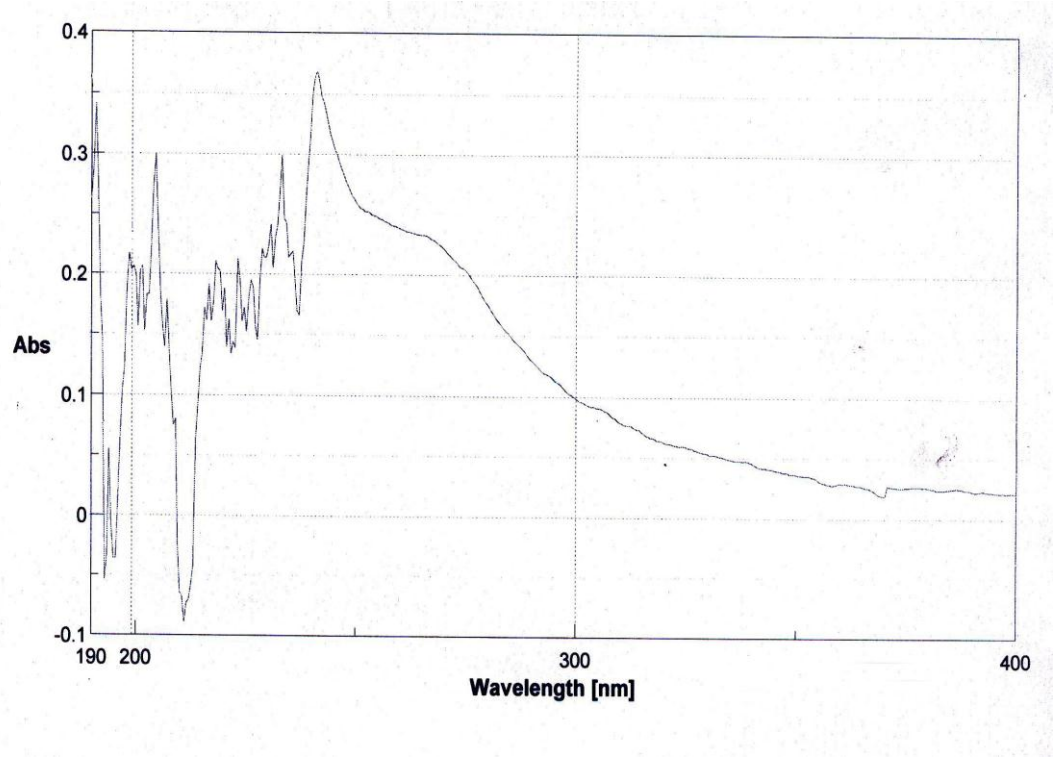

Alexandria *n*-Heptane Aromatics

Figure-30: Ultraviolet Spectra of the n-Heptane Aromatics Separated from Suez and Alexandria Vacuum Residues.

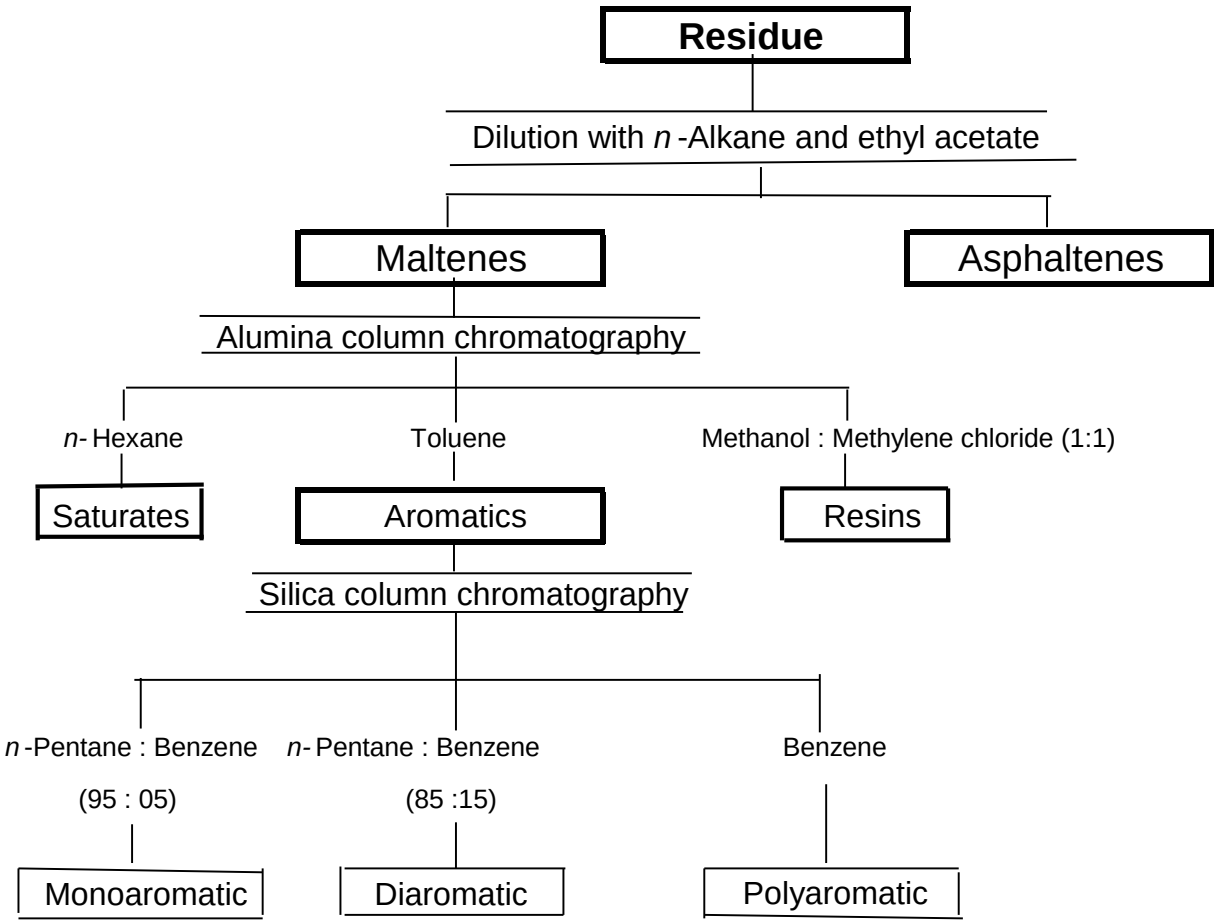

Figure- 31: SCHEME OF SEPARATION OF THE RESIDUE INTO SATURATES, AROMATICS, RESINS AND ASPHALTENES.